The International Center for Theoretical Physics

A Holographic Approach to Boundary CFTs

Author:
Rafael F. Córdoba López

Supervisor:
Prof. Agnese Bissi

High Energy, Cosmology and Astroparticle Physics

23rd August, 2023

Acknowledgments

I would like to express my gratitude to my parents and my brother, who have always supported me to follow my passion for physics. I am also very grateful to my colleagues, who have become more than friends, and to all the professors at ICTP as well as the ICTP staff, who have generously shared their knowledge and guided us throughout this year. I owe a special thanks to my supervisor Agnese, who has been an excellent mentor. I admire your passion for this topic and I am grateful for the opportunity to learn from you and to share your enthusiasm in these topics. Last but not least, I thank Negar, my amazing girlfriend, for the wonderful time we had together and for her love and support. You have made this year so much better. I also thank my flatmates for being there for me and for being part of our new (chaotic) home.

A mi querida tía, que me enseñó a mirar el mundo con admiración, a enfrentar los desafíos con fuerza y valentía, y a vivir cada día con amor y gratitud. Siempre estarás en mi corazón y en mis pensamientos. Esta tesis es para ti, a tu espíritu curioso y a tu sabiduría.

Abstract

In this work, we investigate the holographic approach to the defect crossing equation. More precisely, we use Witten diagrams to study the crossing equation of Conformal Field Theories in the presence of boundaries. We analyze these diagrams and identify the relevant information for the crossing equation. As an example, we compute the Conformal Block decomposition of the boundary and bulk channels in the defect theory and discuss the importance of the results. To first order, we identify that the single trace conformal blocks contributions and the contact diagram conformal block decomposition carries the essential features of the defect crossing equation.

Contents

Introduction

The main subject of study in this thesis is Conformal Field Theories (CFTs) with the presence of boundaries. CFTs are quantum field theories that, besides Poincare invariance, enjoy a larger symmetry group, namely the group of conformal transformations which can be identified to $SO(d+1,1)$, where d is the number of spatial dimensions. Although CFTs enjoy a bigger symmetry group and therefore are more restrictive, they have a lot of interesting applications to study. They arise naturally from fixed points in the renormalization group flow[1], string theory, condensed matter, and quantum gravity, the latter due to the Anti-de-Sitter/CFT (AdS/CFT) correspondence, which states that the (Conformal) field theory is dual to an AdS (quantum) gravity allowing the study of one with the tools of the other [2–7].

On the other hand, CFTs in the presence of a boundary commonly known as boundary CFTs (bCFTs) are a type of a larger class of CFTs called defect CFTs or simply dCFTs. CFTs in the presence of flat defects break the (Euclidean) conformal group $SO(d+1,1)$ into $SO(p+1,1)\times SO(q)$ where p is the dimension of the defect and q its codimension [1, 8–10]. Therefore, the boundary is considered as a flat, co-dimension one defect that constitutes a d dimensional CFT in the bulk together with a $d-1$ dimensional CFT on the boundary rotation symmetric around the boundary. bCFTs are useful for studying conformal field theories in realistic settings, where experimental limitations or boundary conditions break conformal symmetry. They also have theoretical implications for quantum gravity, where a boundary can be interpreted as a D-brane in string theory or the edge of an AdS space. Moreover, bCFTs are often easier to analyze as the insertion of two operators in bCFTs behaves similarly to the insertion of four operators in CFTs, functions that will be our main source of study.

Rather remarkably CFTs are locally characterized by the so-called CFT data

$$\{\Delta_i, C_{ijk}\}_{i,k,l\epsilon I}, \tag{1}$$

this set of information refers to the conformal dimension (Δ) of primaries (the representations of the fields) and the Operator Product Expansion (OPE) coefficients of $\mathcal{O}_i\times\mathcal{O}_j\sim\sum C_{ijk}\mathcal{O}_k$. The importance of the CFT data is that it allows to reconstruct any correlation function of local operators from this piece of information and, therefore, it characterizes CFTs. Indeed, by induction, given an $n-$point function $\langle\mathcal{O}_1\dots\mathcal{O}_n\rangle$ one can perform an OPE expansion among any two fields $\mathcal{O}_i$ and $\mathcal{O}_j$ reducing the $n-$point function to a sum of $(n-1)-$point functions with coefficients completely determined by the CFT data. The process ends with either two or one-point functions which are generally fixed for CFTs, the latter being vanishing due to traditional arguments of conformal invariance (Poincaré invariance and scaling invariance) of the two-point function.

The process, in the presence of a boundary, is the simplest instance of enhancing the CFT data due to nonlocal operators (the codimension $q=1$ defect). In this case, the one-point function may have a non-constant, non-vanishing one-point function and the compatibility conditions pose constraints between boundary and bulk observables, this is due to the symmetry group being broken into a subgroup which does not fix all the information with CFT data. Instead, the scaling dimension of both, the bulk (Δ_i) and boundary ($\hat{\Delta}_i$) fields are needed, together with the OPE of the bulk-bulk $\mathcal{O}^{\text{Bulk}}\times\mathcal{O}^{\text{Bulk}}\sim\sum C\mathcal{O}^{\text{Bulk}}$ and the OPE of bulk-to-boundary $\mathcal{O}^{\text{Bulk}}\sim\sum\hat{C}\mathcal{O}^{\text{Boundary}}$ operators. Therefore, the existence of bulk and boundary OPEs enhances

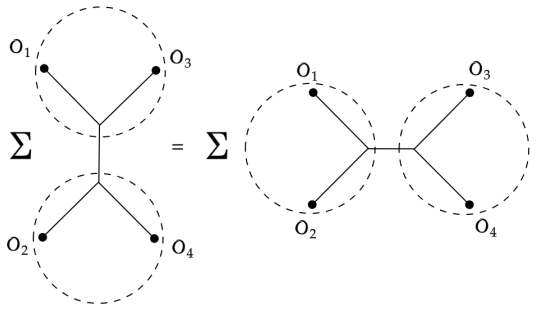

Figure 1: 4-point function OPE expansion crossing symmetry. OPE with (13) and (24) on the left and OPE with (12) and (34) on the right

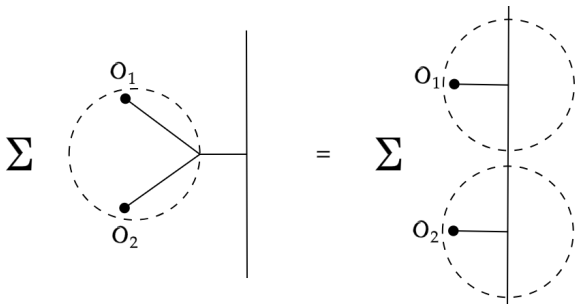

Figure 2: 2-pt function OPE expansion in the defect theory. OPE with bulk operators on the left and OPE with defect operators on the right.

the CFT data to the boundary CFT data,

$$\{\Delta_i, \hat{\Delta}_i, \hat{C}_{ijk}, C_{ijk}\}. \tag{2}$$

The main player of this work is the bootstrap program in which the restrictions of conformal symmetry not only give constraints on the CFT data but allows one to fully determine it [11–13]. The bootstrap procedure encloses consistency conditions on the CFT data through the associativity of the OPEs, it is imposed by the well-known crossing equation

$$1 + \sum \lambda^2_{\Delta,\ell} G_{\Delta,\ell}(u,v) = \left(\frac{u}{v}\right)^{\Delta} \left(1 + \sum \lambda^2_{\Delta,\ell} G_{\Delta,\ell}(v,u)\right) \tag{3}$$

which arises from the 4−point function and schematically showed in Figure 1, in which the computation of a 4−point function can be reduced to a 2−point function of the two possible independent ways of performing the OPE.

Generally, the crossing equation is very restrictive and difficult to manipulate. A simplified yet physically significant example of the bootstrap is the case of bCFTs. In the same spirit as the bootstrap in CFT theory, the presence of a defect constrains greatly two-point functions which, in this case, are not fixed by conformal symmetry but instead are a function of the conformal ratios, the only symmetry invariant quantities in the theory. The associativity is seen, in the two-point functions instead of the four-point function of the usual bootstrap, because of the existence of two different OPEs, the bulk-to-bulk and the bulk-boundary OPEs, pose nontrivial constraints on the CFT data as one can reduce the two-point function to a boundary-boundary or a bulk correlation[14]. Schematically, we have the relation of Figure 2 where the constrained relation resembles the crossing equation in traditional CFTs illustrated in Figure 1. It is one of the goals of our work to exemplify how given a CFT (CFT data) we can give restrictions on the possible defects that the theory may allow, the defect bootstrap is the main tool to do this. In the first part of this work, we formalize the concepts discussed above and derive most of the results stated here. In the second part, we compute some examples of the crossing equation in the presence of a boundary using the AdS/CFT duality and discuss how to extract information from them,

1 Conformal Field Theories

In CFTs local operators at any fixed point in $\mathbb{R}^d$ furnish a representation of the charge algebra $\{Q_\varepsilon\}$ generated by the conformal Killing vectors. This makes the conformal group an extension of the Poincaré group to which we add the generators D and K_μ of dilatations and special conformal transformations respectively. Representations are no longer classified for the two Casimir of the Poincaré group, P^2, and the Pauli-Lubanski W^2, instead, representations are characterized by the new quadratic Casimir which is characterized by the scaling dimension Δ and spin. Our observables $\mathcal{O}$ consist of primaries and descendants. Primaries are defined by operators annihilated by K_μ at 0 and descendants are recursively defined if there exists a primary or descendant $\mathcal{O}'$ such that $\mathcal{O} = P_\mu(\mathcal{O}')$. An additional structure we require in the CFT is the existence of a Hilbert space $\mathcal{H}[S^{d-1}]$ associated with a unitary theory dependent of a S^{d-1} manifold of the foliation $S^{d-1} \times \mathbb{R}$ of the total space. This structure is known as the vector space of local operators at a point.

State-Operator correspondence

Consider a CFT in a flat $d-$dimensional Euclidean theory. Let $x \in \mathbb{R}^d$ be an arbitrary point and parametrize coordinates around this point. Via a Weyl transform the cylinder $\mathbb{R} \times S^{d-1}$ is related to the flat space as

$$ds^2 = dr^2 + r^2 d\Omega_{d-1}^2 = e^{2\tau}(d\tau^2 + d\Omega_{d-1}^2).$$

This means that we can work in the cylinder with radial coordinate in $\mathbb{R}$ being $\tau = \log r$ and we interpret r as the "time" coordinate where dilations generate the evolution of the system. Therefore, a local operator inserted at an arbitrary point in the space is identified as a state at $\tau = -\infty$ in the cylinder. A state on a constant time slice of the cylinder can be propagated backward in time towards $\tau \to \infty$ until it corresponds to a boundary condition on an arbitrary small sphere around the origin which defines a local operator.

The Hilbert space of local operators at a point has an algebraic structure called the Operator Product Expansion (OPE). For the operator $\mathcal{O}(x)\mathcal{O}(0)$ we can perform, due to the state operator correspondence, an evolution to the corresponding state $|\psi(x)\rangle$ which has a (finite) decomposition $\sum_k \lambda_k(x)\,|\mathcal{O}_k\rangle$ as shown in Figure 3. We can organize this decomposition in descendants and primaries as $\sum_{k\ \text{primaries}} C_K(x,P)\,|\mathcal{O}_k\rangle$

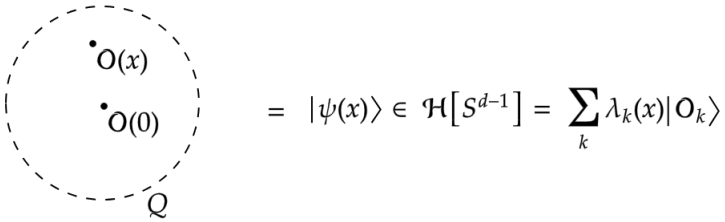

Figure 3: 4-point function OPE expansion crossing symmetry.

which going back at the operator level gives the OPE expansion:

$$\mathcal{O}_1(x)\mathcal{O}_2(x_2) = \sum_{k \text{ primaries}} \lambda_{12}^k C_{12}^k(x_{12}, \partial_y)\mathcal{O}_k(y)\mid_{y=0}, \tag{1.1}$$

where we define $x_{ij} = x_i - x_j$.

1.1 CFTs embedding on the light cone

One of the difficulties of working with CFTs is the nonlinearity of the action of the generators. One way to circumvent this is to embed in a space where the conformal group acts linearly. This is done in the so-called light cone embedding. Take a $d-$dimensional CFT with coordinates x^μ and embeds in the $d+1,1-$ flat space, parametrized by lightcone coordinates (X^+, X^-, X^i) by

$$x^\mu \to (1, x^2, x^i) \tag{1.2}$$

where the metric in the new space is the usual $\mathbb{R}^{d+1,1}$ parametrized by lightcone coordinates $ds^2 = -dX^+dX^- + dX^i dX^j \delta_{ij}$. This make the conformal group to act as $SO(d+1,1)$ group on the embedding space mainly,

$$J_{\mu\nu} = M_{\mu\nu}, \qquad J_{\mu+} = P_\mu, \qquad J_{\mu-} = K_\mu, \qquad J_{+-} = D,$$

where $J_{\mu\nu}$ is the usual generator of $SO(d+1,1)$. Let $\Lambda_N^M \in SO(d+1,1)$ then the action $X \to X' = \tilde{\Lambda}_N^M X^N$ implements the conformal transformations in X by setting that X' is rescaled back to the light cone by $X' = \mathcal{R}(\Lambda X) = (1, x'^2, x'^\mu)$. We impose the fields to satisfy

$$\mathcal{O}(X)|_{section} = \mathcal{O}(x), \quad \mathcal{O}(\lambda X) = \lambda^{-\Delta}\mathcal{O}(X) \tag{1.3}$$

and, additionally, we gauge fix the expression by requiring it to be transversal on the fields

$$X^\mu \mathcal{O}_{\mu\ldots}(X) = 0. \tag{1.4}$$

Condition (1.3) and (1.4) ensures fields are projected to primaries since embedding the physical space in the light cone introduces a bigger ambient space and, therefore, the degrees of freedom of higher spin representations may have differed. The pullback rule gives the projection back to the physical space

$$\mathcal{O}_{\mu\nu\ldots}(x) = \mathcal{O}_{MN\ldots} \underbrace{\frac{\partial X^M}{\partial x^\mu}}_{(0,2x_\mu,\delta_\mu^\nu)} \frac{\partial X^M}{\partial x^\mu}\cdots.$$

This formalism allows to compute easier $n-$point functions as illustrated in the following examples,

Example 1.1.1 (Two point function of spin one fields)**.** *Consider the two-point function $\langle \mathcal{O}_M(X)\mathcal{O}_N(Y)\rangle$. This structure must factorize in scalar and tensor parts. For the scalar, first note that the only Lorentz invariant quantity that this function should depend on is $X \cdot Y$ as $X^2 = Y^2 = 0$ and therefore the two point function is some function $f(X \cdot Y)$. Secondly, by scaling symmetry, f must scale with a power of $-\Delta$ to rescale*

properly meaning that f is a monomial of degree $-\Delta$. We conclude,

$$\langle \mathcal{O}(X)\mathcal{O}(Y)\rangle = \frac{k'}{(X\cdot Y)^{\Delta}}. \tag{1.5}$$

We can set the normalization of the field $\mathcal{O}$ so that $k' = 1$. To project back into physical space we compute

$$X\cdot Y = -\frac{1}{2}(x^2+y^2) + x^\mu y^\nu \delta_{\mu\nu} = -\frac{1}{2}(x-y)^2,$$

therefore, in physical coordinates, the two-point function gives the expected result of free scalar fields. From this is clear that the two-point function of two operators with different scaling dimensions must vanish.

Now, for spin one fields, the most general Lorentz invariant with scaling Δ, transversal to X_M and Y_N is

$$\langle \mathcal{O}_M(X)\mathcal{O}_N(Y)\rangle = \underbrace{\frac{C_{\mathcal{O}\mathcal{O}}}{(X\cdot Y)^{\Delta}}}_{\text{scalar structure}} \times \underbrace{\left(\eta_{MN} + \alpha\frac{X_N Y_M}{X\cdot Y}\right)}_{\text{Tensor structure}}$$

were we identify the scalar structure as in the spin 0 fields and the tensor structure must be a degree zero (in every variable) rank 2 tensor and no terms X_N or Y_M appears by being transversal. Further, being transversal also implies $\alpha = -1$. Having the form of the two-point function we can project into physical space,

$$Y_M \to \frac{\partial X^M}{\partial x^\mu} Y_M = -(x-y)_\mu, \qquad X_N \to \frac{\partial Y^N}{\partial y^\mu} X_M = (x-y)_\mu, \qquad \eta_{MN} \to \frac{\partial Y^M}{\partial y^\mu}\frac{\partial X^N}{\partial x^\nu}\eta_{MN} = \delta_{\mu\nu},$$

where we used $\frac{\partial Y^M}{\partial y^\mu} = (0, 2y_\mu, \delta^\nu_\mu)$. Finally, the two-point function in physical space is

$$\langle \mathcal{O}_\mu(x)\mathcal{O}_\nu(y)\rangle = C_{\mathcal{O}\mathcal{O}}\frac{\delta_{\mu\nu} - 2\frac{(x-y)_\nu (x-y)_\mu}{(x-y)^2}}{(x-y)^{2\Delta}} = C_{\mathcal{O}\mathcal{O}}\frac{I_{\mu\nu}(x-y)}{(x-y)^{2\Delta}}.$$

Spin 1 and 2 fields (e.g. currents and energy-momentum tensor) are expected to be conserved for $\Delta = d-1$ and $\Delta = d$ respectively as there is nothing to be adjusted. Indeed, for the former case, sending $y \to 0$ and requiring conservation gives $2\Delta - 2d + 2 = 0$ or simply $\delta = d - 1$.

Example 1.1.2 (Scalar three-point function with spin)**.** *One step further is to consider the three-point $\langle \mathcal{O}_1(X)\mathcal{O}_2(Y)\mathcal{O}_{3M}(Z)\rangle$ in lightcone space. This function has to factorize in scalar factor times a tensor structure in M. The scalar factor should be proportional to some monomial on the three possible (independent) Lorentz contractions i.e. $X\cdot Y$, $X\cdot Z$ and $Z\cdot Y$ as the coordinates X^2, Y^2 and Z^2 are vanishing. Using the scaling rule and the dimension of the fields we have*

$$\frac{1}{(X\cdot Y)^{\alpha_{123}}(X\cdot Z)^{\alpha_{132}}(Z\cdot Y)^{\alpha_{321}}}$$

where $\alpha_{123} + \alpha_{132} + \alpha_{321} = 2(\Delta_1 + \Delta_2 + \Delta_3)$ by scaling invariance and, by special conformal transformations,

$$\alpha_{123} + \alpha_{132} = \Delta_1, \qquad \alpha_{123} + \alpha_{321} = \Delta_2, \qquad \alpha_{132} + \alpha_{321} = \Delta_3,$$

giving $\alpha_{ijk} = \frac{\Delta_i+\Delta_j-\Delta_k}{2}$.

On the other hand, the tensor structure has to satisfy:

1. *Scaling is* 0 *in all variables (as the scaling is already in the scalar form)*
2. *Transverse,* $Z^M(\text{tensor structure})_M = 0$

Demanding the expression be transversal on Z *variable implies the tensor structure only depends on* X_M, Y_N *and the Lorentz invariant quantities* $X\cdot Y$, $X\cdot Z$, $Y\cdot Z$ *giving* $f(X\cdot Y, X\cdot Z, Y\cdot Z)X_M + g(X\cdot Y, X\cdot Z, Y\cdot Z)Y_M$. *To construct a rank 1, degree* 0 *polynomial we must have the form*

$$\frac{(X\cdot Z)Y_M + \beta(Z\cdot Y)X_M}{(X\cdot Z)^\alpha (Y\cdot Z)^\alpha (X\cdot Y)^\alpha}$$

where we reabsorbed the constant in front of Y_M *into the scalar part. The scaling being* 0 *implies* $\alpha = \frac{1}{2}$ *and contracting with* Z_M *requiring to be transversal implies* $\beta = -1$. *Projecting back gives* $X_M \to (x-z)_\mu$, $Y_M \to (y-z)_\mu$ *and the usual Lorentz contractions,*

$$\langle \mathcal{O}_1(X)\mathcal{O}_2(Y)\mathcal{O}_{3M}(Z)\rangle = \underbrace{\frac{C_{123}}{(X\cdot Y)^{\alpha_{123}}(X\cdot Z)^{\alpha_{132}}(Z\cdot Y)^{\alpha_{321}}}}_{Scalar\ structure} \underbrace{\frac{(X\cdot Z)Y_M - (Z\cdot Y)X_M}{(X\cdot Z)^{\frac{1}{2}}(Y\cdot Z)^{\frac{1}{2}}(X\cdot Y)^{\frac{1}{2}}}}_{Tensor\ structure}. \tag{1.6}$$

Notice that in general the transverse condition can be written in terms of the transverse tensor $C_{MN} = X_N Y_M - X_M Y_N$ *in which case the tensor structure is simply* $\frac{Z^N C_{MN}}{f(X,Y,Z)}$ *where* f *assures that the tensor structure scales as a degree* 0 *polynomial. Going back to physical space,*

$$\begin{aligned}\langle \mathcal{O}_1(x)\mathcal{O}_2(x)\mathcal{O}_{3M}(z)\rangle =& \frac{C_{123}}{(x-y)^{\Delta_1+\Delta_2-\Delta_3}(x-z)^{\Delta_1+\Delta_3-\Delta_2}(z-y)^{\Delta_3-\Delta_2-\Delta_1}} \frac{|y-z||x-z|}{|x-y|}\left(\frac{(x-z)_\mu}{|x-z|^2} - \frac{(y-z)_\mu}{|y-z|^2}\right)\\ \equiv& \frac{C_{123}}{(x-y)^{\alpha_{123}}(x-z)^{\alpha_{132}}(z-y)^{\alpha_{321}}} R_\mu(x,y|z)\end{aligned}$$

this is precisely the only indexed object for three-point functions that transform correctly under conformal transformations.

Finally, this convention allows us to introduce a compact way higher spin fields by encoding them in polynomials:

$$F_{\mu_1\cdots\mu_J}(x) \to F_J(Z,X) = Z^{\mu_1}\cdots Z^{\mu_J} F_{\mu_1\cdots\mu_J} \tag{1.7}$$

subject to $Z^2 = 0$ and $Z\cdot P = 0$ giving $Z = (0, 2x\cdot z, x^\mu)$. Freeing up indices is done by using the Todorov operator:

$$D_\mu = \left(\frac{d-2}{2} + Z^\mu \frac{\partial}{\partial Z^\mu}\right)\frac{\partial}{\partial Z^\mu} - \frac{1}{2} Z_\mu \frac{\partial^2}{\partial Z^\nu \partial Z_\nu}. \tag{1.8}$$

Indices are recovered by the formula

$$F_{\mu_1\cdots\mu_J} = \frac{D_{\mu_1}\cdots D_{\mu_J}}{J!(\frac{d-2}{2})_J},$$

where $(a)_b = \frac{\Gamma(a+b)}{\Gamma(b)}$ is the pochammer symbol.

1.2 The Conformal Bootstrap

Definition 1.2.1 (CFT data)**.** *Consider a CFT whose primaries are labeled by $\mathcal{O}_i$ for some $i \in I$ whose scaling dimension and OPE coefficients are Δ_i and $C_{\mathcal{O}_i\mathcal{O}_j\mathcal{O}_k}$ respectively. The set of data*

$$\{C_{\mathcal{O}_i\mathcal{O}_j\mathcal{O}_k}, \Delta_i\}_{\{i,j,k\}\subset I} \tag{1.9}$$

is called the (local) CFT data. The CFT data contains all the local information of the theory as any $n-$point function can be computed by an inductive process as sketched in the introduction. Further, the coefficient C_{ijk} is related to the 3pt function by

$$\begin{aligned}\langle\mathcal{O}(x_1)\mathcal{O}(x_2)\mathcal{O}(x_3)\rangle &= \frac{\lambda_{\mathcal{O}\mathcal{O}\mathcal{O}}}{|x_1-x_2|^{\alpha_{123}}|x_1-x_3|^{\alpha_{132}}|x_2-x_3|^{\alpha_{231}}} = \sum_{K\ primaries}\lambda_{12}^k C_{12}^K(x_{12},\partial_2)\langle\mathcal{O}_K(x_2)\mathcal{O}(x_3)\rangle \\ &= C_{12}^{\Delta}(x_{12},\partial_2)\frac{1}{|x_2-x_3|^{2\Delta}}\end{aligned}$$

where we used the OPE of Equation (1.1) *to reduce the $3-$pt function into a two-point function and, the orthogonality of primaries with different dimensions. Hence the CFT data is determined by the $3-$pt functions and scaling dimensions of primaries.*

For the case of 4−pt functions, we apply the OPE twice so I can expand in operators at the origin of each circle as shown in Figure 4. This allows a reduction to a 2−pt function and a general function of degree 0 of the cross ratios,

$$\langle\mathcal{O}(x_1)\mathcal{O}(x_2)\mathcal{O}(x_3)\mathcal{O}(x_4)\rangle = \sum_O \lambda^2_{\mathcal{O}\mathcal{O}\mathcal{O}} C_a(x_{12},\partial_{x_2})C_b(x_{34},\partial_{x_4})\langle\mathcal{O}^a(x_2)\mathcal{O}'^b(x_4)\rangle = \frac{f(u,v)}{|x_{14}|^{2\Delta}|x_{32}|^{2\Delta}}, \tag{1.10}$$

where Δ is the scaling dimension of $\mathcal{O}$ and, u and v are the invariant cross ratios

$$u = \frac{x_{12}^2x_{34}^2}{x_{13}^2x_{24}^2}, \qquad v = \frac{x_{14}^2x_{32}^2}{x_{13}^2x_{24}^2}.$$

Definition 1.2.2 (Conformal blocks)**.** *We want to organize the OPE information of the $4-$pt function according to conformal families, more precisely, to $SO(d+1,1)$ representations. The coefficients that carry each family are called conformal blocks giving the decomposition,*

$$f(u,v) = 1 + \sum_{\Delta,\ell}\lambda^2_{\Delta,\ell}G_{\Delta,\ell}(u,v). \tag{1.11}$$

The conformal blocks are general for every theory and the task of computing $4-$pt functions is solely determined by finding the coefficients λ which, in turn, can be found from the OPE coefficients C.

The bootstrap program is based on the observation that one can equivalently do the OPE as shown in the right-hand side of Figure 4 which, in our cross ratios, translates to the $u \leftrightarrow v$ swap. Since these two

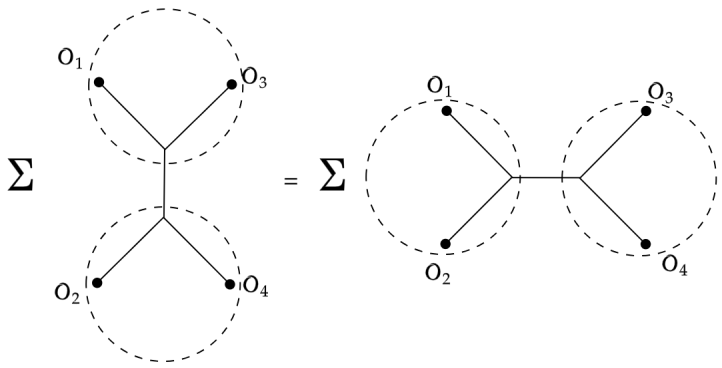

Figure 4: Two different contractions of OPE for a 4-pt function

expressions must agree, we get the consistency conditions:

$$\langle 0|\,\mathcal{O}_1\mathcal{O}_2\mathcal{O}_3\mathcal{O}_4\,|0\rangle = \frac{1}{|x_{12}|^{2\Delta}|x_{34}|^{2\Delta}}\left(1+\sum_{\Delta,\ell}\lambda^2_{\Delta,\ell}G_{\Delta,\ell}(u,v)\right) = \frac{1}{|x_{14}|^{2\Delta}|x_{32}|^{2\Delta}}\left(1+\sum_{\Delta,\ell}\lambda^2_{\Delta,\ell}G_{\Delta,\ell}(v,u)\right).$$

Rearranging the equation, this gives the so-called crossing equation

$$1+\sum\lambda^2_{\Delta,\ell}G_{\Delta,\ell}(u,v) = \left(\frac{u}{v}\right)^{\Delta}\big(1+\sum\lambda^2_{\Delta,\ell}G_{\Delta,\ell}(v,u)\big). \tag{1.12}$$

At the heart of this equation lies the great success of the Bootstrap program. Putting simply, the questions we want to address are: Given a CFT data candidate is this an allowed CFT? The bootstrap equation gives a tool to address this question as it poses great constraints on CFT data which, in turn, can be used to rule out many non-trivial CFT data candidates and even further to solve and construct some theories.

2 Conformal Field Theories and Defects

From now on, we consider our theory as a CFT with a flat p–defect $\mathcal{O}_p$, whose coordinates are $x^\mu = (x^a, x^i)$ with the i components being transverse and a parallel to the defect. The full coordinates in the embedding space split's by $M = (A, I), \quad A = 1,\dots,p+2, \quad I = 1,\dots,q$. In this case the light cone allows the existence of two invariant quantities in the parallel and transverse directions by

$$P \bullet Q = P^A Q^B \eta_{AB} \qquad P \circ Q = P^I Q^J \delta_{IJ}.$$

Notice, however, that since $P^2 = Z^2 = Z\cdot P = 0$ not all contractions are independent. The defect is inserted in the vacuum meaning that our correlation functions take the form

$$\langle X\rangle \equiv \frac{\langle 0|\,X\mathcal{O}_p\,|0\rangle}{\langle 0|\,\mathcal{O}_p\,|0\rangle}$$

where 0 is the vacuum of the CFT theory without the defect and X is any operator combination of bulk and defect operators denoted $\mathcal{O}$ and $\hat{\mathcal{O}}$ respectively.

2.1 Lightning steps

Recall that in the presence of a p–flat defect the conformal group $SO(d+1,1)$ is broken to $SO(p+1,1)\times SO(q)$ with q the codimension of the defect. Hence operators carry labels of scaling dimension and spin of $SO(p)$ and $SO(q)$ denoted by s and j called the transverse and parallel spin respectively. Let J_{MN} be the conformal group generators of the full theory, we know that

$$J_{MN}\left|0\right\rangle = 0, \qquad J_{AB}\left|\hat{D}\right\rangle = J_{IJ}\left|\hat{D}\right\rangle, = 0 \tag{2.1}$$

fixing the vacuum of the CFT and the vacuum of the dCFT. The Casimir operators of $SO(d+1,1)$, $SO(p+1,1)$ and $SO(q)$ are

$$J^2 = \frac{1}{2}J_{MN}J^{MN} \implies J^2\left|\alpha\right\rangle = C_{\Delta,J}\left|\alpha\right\rangle \tag{2.2}$$

$$L^2 = \frac{1}{2}J_{AB}J^{AB} \implies L^2\left|\hat{\alpha}\right\rangle = \hat{C}_{\hat{\Delta},0}\left|\hat{\alpha}\right\rangle \tag{2.3}$$

$$S^2 = \frac{1}{2}J_{IJ}J^{IJ} \implies S^2\left|\hat{\alpha}\right\rangle = \hat{C}_{0,s}\left|\hat{\alpha}\right\rangle \tag{2.4}$$

where $C_{\Delta,J} = \Delta(\Delta-d)+J(J+d-2)$ and $\hat{C}_{\hat{\Delta},J} = \hat{\Delta}(\hat{\Delta}-p)+s(s+q-2)$. In the context of light cone embedding the index-free notation is then encoded in the auxiliary variables Z and W whose corresponding Todorov operators for parallel and transverse directions are

$$D_a = \left(\frac{p-2}{2}+z^b\frac{\partial}{\partial z^b}\right)\frac{\partial}{\partial z^a}-\frac{1}{2}z_a\frac{\partial^2}{\partial z^b\partial z_b}, \qquad D_i = \left(\frac{q-2}{2}+w^j\frac{\partial}{\partial w^j}\right)\frac{\partial}{\partial w^i}-\frac{1}{2}w_a\frac{\partial^2}{\partial w^j\partial w_j}.$$

Therefore, in the lightcone embedding, a general defect operator is written by $\hat{\mathcal{O}}(Z^A,W^I)$ with Z and W the auxiliary variables defined in the index-free notation before. The defect is spatially embedded in the light cone by

$$X^A = (1,x^2,x^a), \quad X^I = 0. \tag{2.5}$$

Following the same notation of the previous section, with coordinates in the light cone described in uppercase, the only two index quantity that assures the transversality condition (cf. Equation (1.6)) is

$$C^{MN} = P^M Z^N - P^N Z^M,$$

which in the presence of the defect splits into C^{AB}, C^{IJ} and, C^{AI}. If there are only bulk insertions then only the last is needed as the other two quantities can be written as a linear combination of that shown in the Equation A.1. We proceed to compute a few $n-pt$ functions to show the embedding formalism in the presence of the defect.

Example 2.1.1 (Two point function of defect operatrors)**.** *Similarly, as we deduced the two-point function*

in general CFTs, the two-point function in the lightcone of the defect operators $\hat{\mathcal{O}}$ is easily seen to be

$$\langle \hat{\mathcal{O}}_{\hat{\Delta},0,s}(P_1,W_1)\hat{\mathcal{O}}_{\hat{\Delta},0,s}(P_2,W_2)\rangle = \frac{(W_1\circ W_2)^s}{(-2P_1\bullet P_2)^{\hat{\Delta}}}$$

as the scaling dependence is encoded in the denominator and the spin-only invariant quantity on transversal fields, each one of spin s, is encoded at the denominator, a result familiar to the two-point function in the general CFT as expected, since the defect operators lie on a CFT by their own. Note that we have chosen the normalization of the fields so that the arbitrary constant in this is 1 and the representation on $SO(q)$ is spin 0 as they lives on the defect. For spin $s=0$ we have,

$$\langle \hat{\mathcal{O}}_{\hat{\Delta}}(x_1^a)\hat{\mathcal{O}}_{\hat{\Delta}}(x_2^a)\rangle = \frac{1}{|x_1^a-x_2^a|^{2\hat{\Delta}}}. \tag{2.6}$$

Example 2.1.2 (One point function of bulk operators)**.** *The story gets more interesting when we consider defect-bulk operators. As mentioned in the introduction, in a CFT without defects the one-point function vanishes in general (except for the identity operator in the bulk), however, in the presence of the defect, we can have, in general, the form*

$$\langle \mathcal{O}_{\Delta,J}(P,Z)\rangle = a_O\frac{Q_J(P,Z)}{(P\circ P)^{\frac{\Delta}{2}}}$$

where Q_J must be a degree J homogenous polynomial in Z, of degree zero in P and transverse. This fixes Q_J to be $Q_J(P,Z)=\left(\frac{C^{AI}C_{AI}}{2P\circ P}\right)^{J/2}=\left(\frac{(P\circ Z)^2}{P\circ P}-Z\circ Z\right)^{J/2}$ where we used the fact that it must depend on the building blocks C^{AI} and expanded the contraction. Conservation implies $\partial_M D^M\frac{Q_J(P,Z)}{(P\circ P)^{\Delta/2}}=0$ which is the condition:

$$J(q+J-3)(d-\Delta+J-2)\frac{P\circ Z}{2(P\circ P)^{\frac{\Delta+2}{2}}}Q_{J-2}(P,Z)=0$$

giving the usual $\Delta=d-2+J$ constrain. For a spin 0 field, going back to physical space gives

$$\langle \mathcal{O}(x)\rangle = \frac{a_{\mathcal{O}}}{|x^i|^{\Delta}}, \tag{2.7}$$

where $a_{\mathcal{O}}$ is some constant not fixed by the symmetries.

Example 2.1.3 (Bulk-defect 2−pt function scalar)**.** *We write the case of two scalars but the full computation for a higher spin is given in Appendix A. In this case, the only independent invariant quantities are $P_1\circ P_1$ and $P_1\bullet P_2$, scaling invariance gives*

$$\left\langle \mathcal{O}_{\Delta}(P_1)\,\widehat{\mathcal{O}}_{\widehat{\Delta}}(P_2)\right\rangle = \frac{b_{\mathcal{O}\hat{\mathcal{O}}}}{(-2P_1\bullet P_2)^{\widehat{\Delta}}\,(P_1\circ P_1)^{\frac{\Delta-\widehat{\Delta}}{2}}}.$$

Projecting back to physical space gives,

$$\langle \mathcal{O}(x)\hat{\mathcal{O}}(0)\rangle = \frac{b_{\mathcal{O}\hat{\mathcal{O}}}}{|x|^{\Delta-\hat{\Delta}}|x^a|^{2\hat{\Delta}}} \tag{2.8}$$

as expected since the bulk operator, close to the extended operator, can be expanded by the defect OPE as

$$\mathcal{O}(x^a, x^i) \sim b_{\mathcal{O}\hat{\mathcal{O}}} |x|^{\hat{\Delta}-\Delta} \hat{\mathcal{O}}(x^a). \tag{2.9}$$

Example 2.1.4 (Bulk-Bulk in the presence of the defect)**.** *Finally, the most important case is the case of two bulk operators. One can think of two bulk operators in the defect theory as four insertions in a theory without defects where the additional points are located in the mirror image of the defect i.e. in the coordinates* $\bar{x} = (x^a, -x^i)$*. Indeed, in this case, there are two independent "cross ratios" (cf. with four-point function cross ratio) of the form*

$$\xi_1 = \frac{(x_1 - x_2)^2}{4|x_1^i||x_2^i|}, \quad \xi_2 = \cos\alpha = \frac{x_1^i \cdot x_2^i}{|x_1^i||x_2^i|}, \tag{2.10}$$

the first one is easily understood as the only Lorentz-rotation ratio of invariants in the theory. The second is an invariant under rotations as exemplified in Figure 5. Notice also that the cross ratios are invariant under $x \to \bar{x}$ *implying that the mirror points acquire the same invariant. Bulk-defect* 2*−point functions, therefore,*

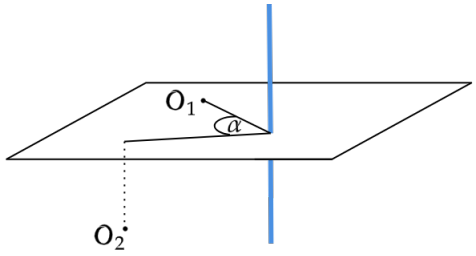

Figure 5: Bulk defect operators in the bulk, the invariant quantities are showed

have more freedom and are expected to depend on a general function $f(\xi_1, \xi_2)$ *of the cross ratios, similar to* 4*−pt functions in CFTs. For this, the only independent invariant quantities are* $P_1 \circ P_1$ *and* $P_2 \circ P_2$*, giving*

$$\langle \mathcal{O}_1(x_1)\mathcal{O}_2(x_2)\rangle = \frac{f(\xi_1, \xi_2)}{|x_1^i|^{\Delta_1}|x_2^i|^{\Delta_2}}. \tag{2.11}$$

This result is one of the most important as it will allow us to perform conformal block expansion in either bulk or defect conformal blocks imposing restrictions on the theory.

Remark 2.1.1. *Notice that for the case of boundaries, we have only one perpendicular coordinate* $x^i = r$*. In this case, we have only one cross ratio* ξ_1*.*

2.2 The defect conformal bootstrap

Under an insertion of a p−dimensional defect, the CFT data is enhanced. This is due to the appearance of defect operators $\hat{\mathcal{O}}(x^a)$ parametrized with coordinates parallel to the defect, correlations of bulk-bulk operators, and, correlations of bulk-defect operators. The CFT data is, therefore, enhanced to

$$\{C_{ijk}, \hat{C}_{ijk}, \Delta_i, \hat{\Delta}_i\}. \tag{2.12}$$

Using the two-point function we can either expand with bulk or defect conformal blocks as schematically shown in Figure 6. Indeed, using the OPE of two primaries in the bulk we can compute the LHS of Figure

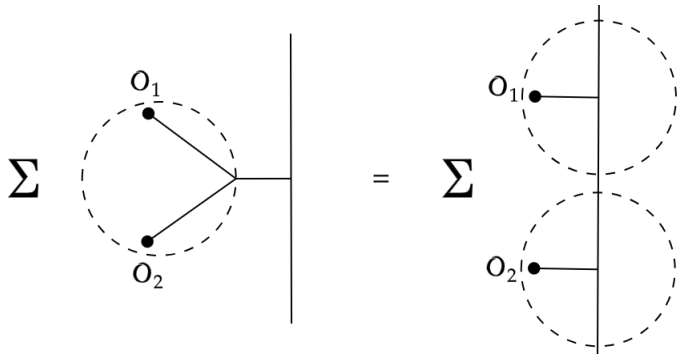

Figure 6: OPE expansion in the defect theory. OPE with bulk operators on the left and OPE with defect operators on the right

6 giving the two-point function,

$$\begin{aligned}\langle \mathcal{O}_1(x_1)\mathcal{O}_2(x_2)\rangle &= \sum_{\Delta,I} \lambda_{\Delta,I} C_{\Delta,I}(x_{12},\partial_y)_{|_{y=0}} \langle \mathcal{O}_{\Delta,I}(y)\rangle = \sum_{\Delta,I} \lambda_{\Delta,I} C_{\Delta,I}(x_{12},\partial_y)_{|_{y=0}} \frac{a_\Delta}{r_y^\Delta} \\ &= \frac{1}{r_1^{\Delta_1} r_2^{\Delta_2}} \left(\sum_{\Delta,I} \lambda_\Delta a_\Delta G^{\text{bulk}}_{\Delta,I}(\xi_1,\xi_2) \right)\end{aligned}$$

where we used the 1−pt function in the defect theory (Equation (2.7)) and defined the conformal block in the bulk G^{bulk} that depends on ξ_1 and ξ_2, the invariant cross ratios of Equation (2.10). To compute this conformal block in the case of a codimension one defect (boundary), we use the Casimir trick (for a $(d-1)$ dimensional space), outlined in Appendix B.1, that shows that the CBs are eigenstates of the Casimir. In this case, the coefficients Δ, I run over all primaries admitted in $\mathcal{O}\times\mathcal{O}$ with non-vanishing one point functions. In particular, for the codimension $q=1$ defect only scalars are allowed and, solving the eigenstate (differential) equation, we find the CBs to be:

$$G^{\text{bulk}}_\Delta(\xi_1) = \frac{\xi_1^{\frac{\hat\Delta}{2}}}{\xi_1^\Delta} {}_2F_1\left(\frac{\hat\Delta}{2},\frac{\hat\Delta}{2},1-\frac{d}{2}+\hat\Delta,-\xi_1\right), \tag{2.13}$$

where we recall $\xi_2 = 1$ and ${}_2F_1$ is the hypergeometric function. On the other hand, since the OPE with the defect is $\mathcal{O}(x) = \sum_\Delta \lambda_{\hat\Delta,I} \hat{C}_{\hat\Delta,I}(r,\partial_y)_{|_{y=0}} \hat{\mathcal{O}}_I(y)$ then, plugging in the two-point function gives,

$$\langle \mathcal{O}_1(x_1)\mathcal{O}_2(x_2)\rangle = \sum_{\hat\Delta,I} \lambda^2_{\hat\Delta,I} \left[\hat{C}_{\hat\Delta,I}|_{y=0}(r_1,\partial_y) C_{\hat\Delta,I}|_{z=0}(r_2,\partial_z)\right] \langle \hat{\mathcal{O}}_{\hat\Delta,I}(y)\hat{\mathcal{O}}_{\hat\Delta,I}(w)\rangle \tag{2.14}$$

$$= \frac{1}{r_1^{\Delta_1} r_2^{\Delta_2}} \left(\sum_{\hat\Delta,I} \lambda^2_{\hat\Delta,I} G^{\text{defect}}_{\Delta,I}(\xi_1,\xi_2) \right), \tag{2.15}$$

where we defined the conformal block in the defect theory. Note that in contrast to the G^{bulk} which is eigenfunction of the Casimir operator of the full $SO(d+1,1)$ here the conformal block is eigenfunction of the casimir in the $SO(p,2)\times SO(q)$. The Casimir equation for defect channel splits into each of the direct product Casimirs $S^2 = \frac{1}{2}(J_{IJ})^2$ and $L^2 = \frac{1}{2}(J_{AB})^2$ giving a system of differential equations for the defect

channel conformal block that can be found in the Appendix B.2. We solve this system of equations to find the defect conformal blocks which, for a codimension 1 flat defect, we call the boundary conformal blocks. The boundary conformal blocks, however, can be computed explicitly from the OPE! See the Appendix of [15] for a derivation of this. This gives:

$$G_{\Delta}^{\text{Boundary}}(\xi_1) = \frac{1}{\xi_1^{\hat{\Delta}}}{}_2F_1\left(\hat{\Delta}, 1-\frac{d}{2}+\hat{\Delta}, 2-d+2\hat{\Delta}, -\frac{1}{\xi_1}\right). \tag{2.16}$$

We conclude that the coefficient expansion $\lambda_{\hat{\Delta}}$, a_Δ and λ_Δ must satisfy, for a boundary defect, the defect crossing equation:

$$\sum_{\Delta,I} \lambda_{\Delta,I} a_\Delta G_{\Delta,I}^{\text{bulk}}(\xi_1) = \sum_{\hat{\Delta},I} \lambda_{\hat{\Delta},I}^2 G_{\Delta,I}^{\text{defect}}(\xi_1). \tag{2.17}$$

Remark 2.2.1. *The coefficients of the RHS are definite positive while the coefficients on the bulk side may be either sign. This, in turn, is different from the crossing equation 4 as, in this case, both sides are positive definite.*

In contrast to the Ward identities, the defect conformal bootstrap will give rise to many constraints and therefore looks more promising as a tool to constrain the CFT data. The downside is that these restrictions are not manifest and it may be difficult to find explicit relations among coefficients because the pairing between coefficients on the right and left side can, in principle, be one to an (infinite) family of blocks. We turn our attention to this tool as it is not only more powerful but recent progress has been made into harnessing more information from bootstrap techniques.

Example 2.2.1. *Generally, the defect crossing equation is very difficult to solve and few instances of solutions are known [13, 14]. Rather surpassingly, there is an easy solution to this equation found in [14]. In the limit where $\xi_1 \to 0$ we can expand in power series both sides, $G^{Bulk} = \left(\frac{\xi}{1+\xi}\right)^{\Delta}$ and $G^{Boundary} = c_1(1+\dots) + c_2\xi^{1-d/2}$. Matching the power of ξ_1 on left and right side we get $\Delta = \frac{d}{2} - 1$ and $\eta = 2\Delta = d-2$. This is, the scaling dimension of the free field. Expanding around $\xi_1 \to \infty$,*

$$1 + \lambda_\eta a_\eta \left(1 + \frac{1-d/2}{\xi} + \dots\right) = \xi^{\Delta}\left(a_O^2 + \mu^2 \xi_1^{-\hat{\Delta}}\left(1 - \frac{\hat{\Delta}}{2\xi} + \dots\right)\right).$$

We choose $\lambda_\eta a_\eta = \pm 1$, $a_O = 0$, $\hat{\Delta} = \Delta$ or $\Delta + 1$, $\lambda^2 = 2$ or $(d-2)/2$. Surpassingly these solutions hold order by order giving the two-point function:

$$\langle \mathcal{O}_1(x)\mathcal{O}_2(x_2)\rangle = \frac{1}{|x_1 - x_2|^{2\Delta}} \pm \frac{1}{|r_1 - r_2|^{2\Delta}}$$

corresponding to Dirichlet and Neumann boundary conditions for the free scalar field[8–10].

3 The Boundary Bootstrap from Holography

In this section we show how the crossing equation can be approached in holographic CFTs in the presence of a boundary, to do so we rely on the ideas of AdS/CFT correspondence. Although the AdS/CFT is a

very powerful and interesting topic on its own, we will not say much about it as it will deviate ourselves from the main point of this work. Instead, we first define the class of CFT that admits a holographic correspondence mainly, the large N limit CFT, and introduce the main computational tool to work in the (quantum) gravitational side of AdS. Finally, we connect these results with the CFT data finding the first contribution of the conformal blocks. It is worth saying explicitly that our approach to the correspondence is therefore bottom-up in which we give the possible constraints on what the holographic theories with defects must follow instead of explicit realizations of the correspondence.

3.1 CFTs at large N

Consider a $U(N)$ gauge theory with fields valued in the adjoint representation. We can write the action as

$$S = \frac{1}{g_{YM}^2}\int dx\,\mathrm{Tr}\left[-\frac{1}{2}(\partial_\mu\Phi\partial^\mu\Phi) + \Phi^3 + \Phi^4 + \dots\right]$$

For this theory, the one-loop beta function gives the famous beta function

$$\beta(g) = -\frac{g^3}{48\pi^2}\left(11N - 2N_f\right) \tag{3.1}$$

with $N_f = 0$. The beta function diverges at $N \to \infty$, however, if we set $\lambda = g_{YM}^2 N$, $g(\lambda)$ is non vanishing as long as we kept fix λ. In this case, the renormalization group equation becomes

$$\mu\frac{d\lambda}{d\mu} = -\frac{1}{24\pi^2}\lambda^2 + O(\lambda^3),$$

meaning that our theory is not trivial in the large N limit. For this theory the propagator of an adjoint field obeys

$$\left\langle \Phi^i_j \Phi^k_l \right\rangle = \frac{\lambda}{N}\frac{\delta^i_l\delta^k_j}{4\pi^2(x-y)^2}.$$

Thus, Feynman diagrams are double line graphs with vertices scaling as $\frac{N}{\lambda}$ and propagators scaling as the inverse of this. Graphs are then determined by Vertices (V), Loops (F), and Edges (E) giving a total graph scaling

$$N^\chi \lambda^{E-V},$$

were we recognized the Euler characteristic ($\chi = V - E + F = 2 - 2g'$ with g' the genus of the graph) from the N scaling. Therefore, any physical quantity is expressed as an expansion of N and g which are dominated by the genus 0 ($\chi = 2$) graphs called planar graphs.

Definition 3.1.1. *Observables are constructed out of gauge invariant operators. A special case that we will encounter often are the Single Trace (ST) and Double Trace (DT) operators, general ST operators are defined by spin l and grading n by $[\mathcal{O}_i]_{n,l} \sim \partial^{2n}\partial_{\mu_1\dots\mu_l}\mathcal{O}_i$ and have scaling dimension $\Delta_i + 2n + l + \gamma_i(n,l)$ where γ is the anomalous dimension. Similarly, DT operators are defined by $[\mathcal{O}_i\mathcal{O}_j]_{n,l} \sim \mathcal{O}_i\partial^{2n}\partial_{\mu_1\dots\mu_l}\mathcal{O}_j$ and have dimension $\Delta_i + \Delta_j + 2n + l + \gamma_{i,j}(n,l)$. Multitrace operators are defined analogously.*

Remark 3.1.1. *Conformal block decompositions are then labeled by multi-trace operators depending on (n,l).*

A single trace composition then reads $\sum \lambda^2_{[\mathcal{O}_i]_{n,l}} G_{\Delta_i+2N+l+\gamma}$, *while double trace operators are* $\sum \lambda^2_{[\mathcal{O}_i\mathcal{O}_j]_{n,l}} G_{\Delta_i+\Delta_j+2N+l+\gamma_{i,j}}$.

Now, consider a single trace operator. Using the large number of degrees of freedom ($\mathrm{tr}\{\delta_i^j\} = N$) and, adapting the argument above, we can conclude that the connected correlators are given by a large N expansion of the form

$$\langle \mathcal{O}_1 \dots \mathcal{O}_n \rangle_c = \sum_{g'=0}^{\infty} N^{2-n-2g'} f_{g'}(\lambda), \tag{3.2}$$

which is dominated by the planar diagrams ($g' = 0$). We say that this theory enjoys large N factorization as the planar 2−pt function contribution is independent of N while connected higher point functions are suppressed by powers of N. This implies that the 2−pt function of multitrace operators $\tilde{\mathcal{O}}$ is dominated by the product of the two-point functions of its single-trace constituents:

$$\langle \tilde{\mathcal{O}}(x)\tilde{\mathcal{O}}(y)\rangle \approx \prod_i \langle \mathcal{O}_i(x)\mathcal{O}_i(y)\rangle = \frac{1}{(x-y)^{2\sum_i \Delta_i}}.$$

We conclude that the scaling dimension of the multi-trace operator $\tilde{\mathcal{O}}$ is given by

$$\Delta_i = \sum_i \Delta_i^{(0)} + g\Delta_i^{(1)} + \dots$$

and, the OPE coefficients are also decomposded by

$$C_{ij}^k = C_{ij}^{k\,(0)} + gC_{ij}^{k\,(1)} + \cdots$$

with $g \sim 1/N$. This implies that the crossing equation must hold order by order in $1/N$. This is the form of large N factorization that admits a dual interpretation by the AdS/CFT prescription.

Example 3.1.1. *In general, our OPE expansion of single trace operators will be of the form* $\mathcal{O}_1(x)\mathcal{O}_2(0) \sim |x|^{\Delta_1+\Delta_2} \sum_k \mathcal{O}_k |x|^k +$ *descendants. We will see later that the conformal block decomposition of the* $4-$*pt function is given by operators of dimension* $2\Delta + 2n$ *at order zero in* $1/N$*, of single trace operators at order* $1/N$ *and of double trace operators in order* $1/N^2$*. This gives the OPE:*

$$\mathcal{O}_1(x)\mathcal{O}_2(0) \sim \frac{1}{x^{\Delta_1+\Delta_2}}\left[g\sum_k C_k\mathcal{O}_k x^{\Delta_k} + \sum_{i,j,n,l}\left(\delta_{i(1}\delta_{2)j}\left(C_{n,l}^{'(i,j)} + g^2 C_{n,l}^{''(i,j)}\log x\right) + g^2\right) C_{n,l}^{(i,j)}\mathcal{O}_{n,l}^{(ij)} x^{\Delta_i+\Delta_j+2n+l}\right]. \tag{3.3}$$

where C_k, $C^{(i,j)}$, $C^{'(i,j)}$ *and,* $C^{''(i,j)}$ *are now, in principle, order zero constants and, we also include the logarithmic term for future convenience. This term corresponds to the factor that emerges from the corrections to the conformal dimensions of the two-particle operators and, since the terms in brackets must have scaling* 0*, then double trace contributions will resum to cancel this term.*

Definition 3.1.2 (Generalized Free Field)**.** *Generalized Free Fields (GFF) are fields whose* $n-$*pt functions Wick-factorize and can have any conformal dimension. Therefore, in the large N factorization, at zero order in* $1/N$*, the theory is made of GFFs. A solution of the boundary crossing equation can be found in Appendix B.6 of [11].*

3.2 The AdS/CFT correspondence

One of the most important observations in the past few years is that the number of symmetry generators of the conformal group is precisely the same as the number of generators of the $SO(2,d)$. Giving hints that there is a manifold in $d+1$ dimensions that realize the $SO(2,d)$ as isometries, no more, no less! The heart of this observation relies upon the AdS/CFT correspondence. A topic that has changed our understanding of quantum field theories as it allows us to study CFTs from a gravitational perspective or the other way around. The correspondence between $AdS_{d+1} \leftrightarrow CFT_d$ generally relates:

- Isometries of AdS $\leftrightarrow$ Conformal isometries of the boundary of AdS (∂AdS)
- Quantum field theories in AdS_{d+1} with CFT on ∂AdS_{d+1}, where fields on the bulk are related to the CFT operators in the boundary $\hat{\phi}_{AdS}(\rho, x) \leftrightarrow \hat{\mathcal{O}}_{CFT}(x)$.

In terms of correlation functions, the AdS/CFT correspondence relates the gravitational side action with the generating functional of connected graphs in the CFT side by

$$W[\phi_0] = \mathcal{S}_{gravity}\,|_{\lim_{z\to 0}(\phi^{\text{Bulk}} z^{\Delta-d}) = \phi^{\text{Boundary}}(x)}\,. \tag{3.4}$$

Now we are in position to discuss the relation between the 4−pt functions and the CB from the holographic perspective. Consider a free bulk theory, we can add local interactions in the bulk to perturb the theory. If we assume that the n−pt functions on the boundary are still related to correlators in the bulk by the AdS/CFT prescription then the perturbed CFT $n-pt$ functions will be related to the "Witten diagrams" in the bulk, the analogous of Feynman diagrams in curved space-time. For example, turning a $\phi_1\phi_2\phi_3$ interaction in the gravity side will correspond to a nonzero boundary 3−point function $\langle \mathcal{O}_1\mathcal{O}_2\mathcal{O}_3\rangle$ where the three operators $\mathcal{O}_i$ on the boundary are dual to fields ϕ_i for each i in the bulk. Thus, Witten diagrams (together with Equation 3.4) are the main tool to compute n−pt functions on the gravity side, the rules to construct them are the following:

Rules for Witten Diagrams

- The external sources $\phi_{(0)}$ of composite gauge invariant operators $\mathcal{O}$ on the field theory are located at the conformal boundary of AdS spacetime which is represented as the boundary of each circle in Figure 9. The bulk of AdS is represented by the interior of the figure.
- Propagators depart from external sources to either another boundary or to an interior interaction point. In this case, they are called boundary-to-boundary or bulk-to-boundary propagators respectively.
- The structure of the interior interaction points is governed by the interaction terms in the gravity action.
- Two interior interaction points may be connected by bulk-to-bulk propagators.
- Every interaction point in the bulk is integrated over so that the expression is $SO(d+2,1)$ invariant on AdS.

3.3 CFTs at large N in the gravity side

Recall that the 4–pt function depends on a general $f(u,v)$ by

$$\langle \mathcal{O}(x_1)\mathcal{O}(x_2)\mathcal{O}(x_3)\mathcal{O}(x_4)\rangle = \frac{f(u,v)}{|x_{12}|^{2\Delta}|x_{34}|^{2\Delta}}$$

with u and v the conformal rations:

$$u = \frac{x_{12}^2 x_{34}^2}{x_{13}^2 x_{24}^2}, \qquad v = \frac{x_{14}^2 x_{32}^2}{x_{13}^2 x_{24}^2}.$$

Setting $|x_4| \to \infty$, $|x_3| \to 1$, and $x_1 \to 0$, we can choose the coordinates $z = x_1 + ix_2$ and rewrite $u = |z|^2$ and

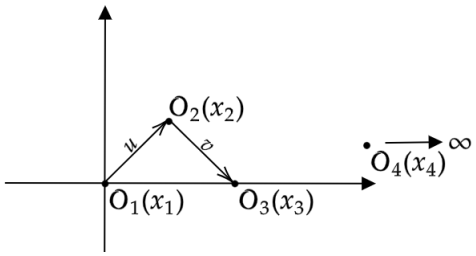

Figure 7: Cross ratio functions u and v in the complex plane, we sent $|x_4| \to \infty$, $|x_3| \to 1$, and $x_1 \to 0$.

$v = |1-z|^2$ as shown in the Figure 7. In this coordinates we can retrieve the different channels limits, for the s–channel we set $u \to 0$ in which case the contributions are composed, to leading order (as seen in Equation (3.7)), of the s–channel diagrams. Similarly, if we set $v \to 0$ this sets the t–channel and, finally the u–channel is set by $u, v \to \infty$.

We consider the 4–pt function of a CFT on the gravity side. This amplitude, at the level of a large N CFT, can be expanded in powers of $\frac{1}{N}$ giving

$$f(z,\bar{z}) = f^{(0)}(z,\bar{z}) + \frac{1}{N^2} f^{(1)}(z,\bar{z}) + \frac{1}{N^4} f^{(2)}(z,\bar{z}) + \dots \tag{3.5}$$

where we use the fact that the N scaling only admits even powers by Equation (3.2). The decomposition is made of the Witten diagrams shown in Figure 8. At zero order on $\frac{1}{N}$ we have only the disconnected

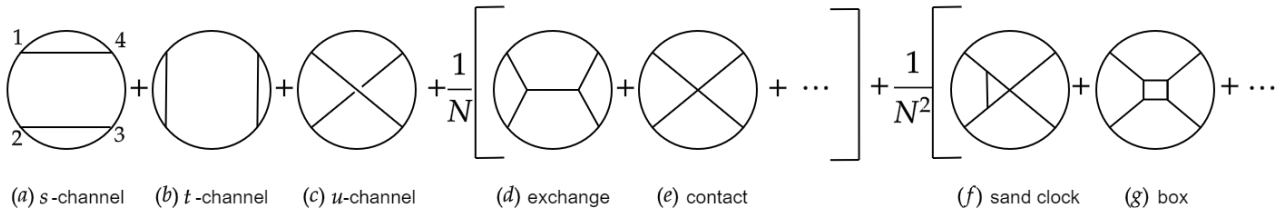

Figure 8: 4pt function Holographic Witten diagrams

pieces meaning that all interactions are turned off and, therefore, retrieving the generalized free fields, as the functions factorize piece-wise. Higher orders give corrections to those.

To see the constraints in the bootstrap Equation 1.12 the question now amounts, once the diagrams are computed, to how to decompose the graphs in terms of the conformal blocks of a fixed channel. To do so we first introduce a technique where it allows us to identify the operator dependence on each Witten diagram in terms of multi-trace operators. This is done by a "cutting rule"[4, 16–19].

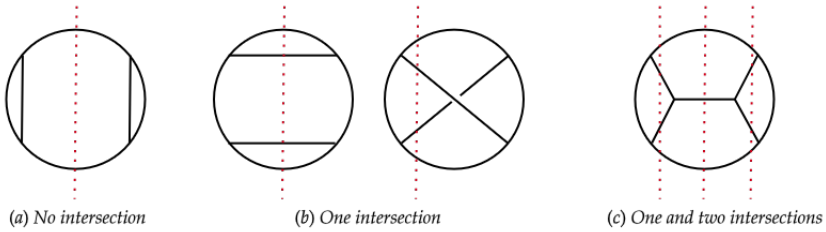

Figure 9: Cutting of Witten diagrams

Cutting rule: CFT decomposition of Witten diagrams for the $s-$channel

For each graph, we perform a transversal cut, shown by a red dotted line in Figure 9. The total number of intersection tell us which kind of operators will contribute to the CB expansion. If the transversal cut does not meet any line then we expect a single operator, an identity being exchanged (free case). If it intersects once, a single trace operator will appear on the expansion, if it intersects twice, a double trace operator contribution may be present and, more intersections are defined analogously. The cut is taken in each possible vertical line that the bulk point being integrated over may cross. The t and s channel decomposition can be seen similarly by taking the relevant cuttings. The proof can be found in [17].

Example 3.3.1. *An exchange Witten diagram, Figure 9 c), will have double trace and single trace operators. This is due to the line intersecting twice at the bulk-boundary propagators and once at the bulk-bulk propagators.*

Therefore, back to the 4−pt function, at the level of CFT and using the decomposition at the $s-$channel limit i.e. taking $z \to 0$ and $\bar{z} \to 0$, the graphs of Figure 8 are schematically expanded by an insertion of identity and sum of double trace operators,

$$f(z,\bar{z}) = 1 + \sum_{n=0}^{\infty} \sum_{l \in 2\mathbb{N}} \lambda_{\mathcal{O}\mathcal{O}[\mathcal{O}\mathcal{O}]_{n,l}} G_{\Delta_i+\Delta_j+2n+l} + O\left(\frac{1}{N}\right) \tag{3.6}$$

and are shown pictorially in Figure 10. Indeed, we can check by computing the disconnected diagrams of the $4-pt$ function expansion,

$$\text{Disconnected Witten diagrams} = \frac{1}{x_{12}^{2\Delta} x_{34}^{2\Delta}} + \frac{1}{x_{14}^{2\Delta} x_{32}^{2\Delta}} + \frac{1}{x_{13}^{2\Delta} x_{24}^{2\Delta}} = \frac{1}{x_{12}^{2\Delta} x_{34}^{2\Delta}} \left[1 + \left(\frac{u}{v}\right)^{\Delta} + u^{\Delta} \right], \tag{3.7}$$

where we used the result that a one-line, boundary-to-boundary Witten diagram, gives the CFT free two

point function, see [3] for a derivation. This implies that the first term of f, in the $s-$channel, is

$$f^{(0)}(z,\bar{z}) = 1 + \left(\frac{z\bar{z}}{(1-z)(1-\bar{z})}\right)^{\Delta} + (z\bar{z})^{\Delta},$$

where the first contribution is the diagram $a)$, the second is the diagram $b)$ and the third is the diagram $c)$ of Figure 8. We see that the cutting rule prediction match our results as the $s-$channel at first order (in the $s-$channel with $z,\bar{z} \to 0$) is simply 1, giving only one term with identity being the exchanged field. At the second order, we have $2(z\bar{z})^{\Delta}$, i.e. the dimension of two external $\mathcal{O}$ each having dimension Δ, the lightest double trace composite of external operators. The coefficient of the amplitudes are precisely the ones in the CB decomposition $C^2_{\mathcal{O}\mathcal{O}[\mathcal{O}\mathcal{O}]_{n,l}}$. Notice that here we see explicitly that the $t/s-$channel contributions are related to an infinite number of (double trace) operators in the $s-$channel expansion and therefore we justify the appearance[1] of double trace operators on the OPE 3.3.

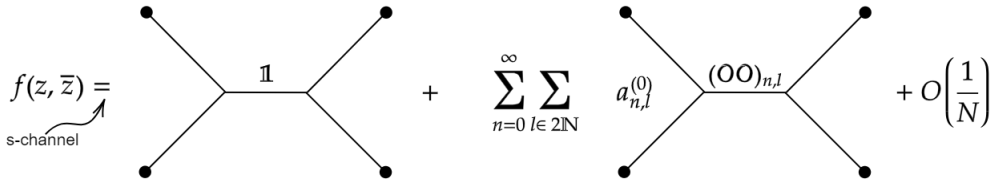

Figure 10: 4pt function dual interpretation CFT, the disconnected diagrams of $a)$, $b)$ and $c)$ of Figure 8 explicitly shown in Equation (3.6) are pictorially represented.

Remark 3.3.1. *Notice that order by order Witten diagrams are manifestly crossing symmetric as we are summing over all the possible channels. Indeed, using Equation* (3.7) *and the analogous for the $t-$channel we have,*

$$\underbrace{1 + \left(\frac{u}{v}\right)^{\Delta} + u^{\Delta}}_{s-channel} = \left(\frac{u}{v}\right)^{\Delta} \underbrace{\left(1 + \left(\frac{v}{u}\right)^{\Delta} + v^{\Delta}\right)}_{t-channel}$$

satisfying the crossing equation. Next order diagrams contribute to perturbations around the GFF but is important to understand how the DT and ST contributions come into play in the crossing equation.

3.3.1 Witten diagrams and the crossing equation

Even though the Witten diagrams will manifestly be consistent with an OPE and the crossing symmetry (as we are summing over all the channels and all possible interactions), they might not recreate a full consistent CFT. Unitarity, as seen by the positivity of the coefficients of the CB expansion, might be violated and further, the effective Witten diagrams might not even allow the OPE coefficients to be real. In this view, only a subset of effective Witten diagrams does retrieve a consistent CFT. One advantage of the introduction of the defect crossing Equation (2.17) is that unitarity imposes positivity of the coefficients in the defect

[1] Technically this only justifies the the appearance of the $[OO]_{n,l}$ operators as they are the only ones that contribute at this level. General contributions are seen, for example, in the DT decomposition of exchange or contact diagrams.

conformal block decomposition and reality is posed in the bulk conformal block decomposition making them at least, in the effective gravitational side, more tamed.

One would expect the exchange diagram in Figure 8 d) to be dual to the conformal block corresponding to the exchange of the (dual) operator with dimension Δ (where $m_\phi^2 = \Delta(\Delta - d)$ by the usual AdS/CFT prescription) and all of its descendants[16–18]. However, their CB decomposition dictates this is the conformal block of the exchanged field plus additional double trace operators, which, as seen in the gravity side, are the leading contribution of the 2−particle states. In this case, the single graph is not crossing symmetric as the t channel contains only double trace CBs and the s−channel contains the single trace CB and a sum of double traces. To see that crossing symmetry is not possible to fulfill, it amounts to (try to) express the single CB G_Δ as a sum of the crossed channel CBs. It turns out that this is not possible for if the operator exchanged is not the identity i.e. there is no exchange then, the conformal block G_Δ expanded in the crossed channel has logarithmic terms in the conformal cross-ratios[16]. This logarithmic behavior is inconsistent with an OPE expansion in the crossed channel, since at this order there are no contributions of anomalous dimensions which might introduce logarithmic dependence. In contrast to the exchange diagram, the contact diagram is compatible with crossing symmetry as the decomposition in both, s and t channels, are made of double trace operators.

The above discussion implies that the problem of satisfying the crossing equation can be reduced to finding the diagrams that contribute to the crossing symmetry of a given diagram. To see this, we use the OPE expansion of Equation 3.3 in which we see the relevant contributions of the CBs order by order in the crossing equation. For example, for the exchange in the s−channel (Figure 8 d)) we see that there is no possible contraction at order less than g^2. At order g^2 we can contract the g^2 DT operator on one side with a g^0 on the other side of the $4-pt$ function or we can contract the order g ST operators on both sides. The crossing equation therefore, in order g^2, must be constructed only by these operators which, in principle can appear in any of the Figure 8 diagrams. Going to the next orders in Figure 8 we don't express the crossing equation but instead, give the schematic contributions:

1. Diagram d): In this case, the CB decomposition depends on the channel. If we take the $s-$ channel, the cutting rule gives single trace and double trace operators. If we choose $t-$ and $s-$channel there are only double trace operators.

2. Diagram e): This type of diagram is called contact. An example of interaction on the gravity side is a ϕ^4 term. Since this is a contact term there is no single trace exchange in the boundary associated with a CFT. This, instead, corrects the double trace corrections of the OPE coefficient. Through the s−channel we have $[\mathcal{O}_1\mathcal{O}_2]_{n,l}[\mathcal{O}_3\mathcal{O}_4]_{n,l}$ and analogously for t and u channel.

3. Diagram f): The double trace operators in the order $O(\left(\frac{1}{N}\right)^0)$ are corrected away from its GFF value. This gives, for example, the anomalous dimensions,

$$a_{n,l} = a_{n,l}^{(0)} + \frac{1}{N}a_{n,l}^{(1)} + \cdots, \qquad \gamma_{n,l} = \frac{1}{N}\gamma_{n,l}^{(1)} + \cdots$$

   where $\gamma_{n,l}$ is the anomalous dimension. This is not only of physical interest but is computationally easy to extract the anomalous dimension. In the CB expansion they come, schematically, as the coefficients

of the CB expansion,

$$G_{\Delta,l} \sim u^{\frac{\Delta-l}{2}}(1+\gamma\log h).$$

We refer to [2, 15, 20, 21] for these relations and how to find them. This diagram has only double trace operators.

4. Diagram g): There are double and higher contributions.

We conclude by summarizing that disconnected graphs reproduce the GFF, the planar (connected) are of two kinds, exchange and contact where the second give purely decomposition of double trace operators. Higher orders give quantum corrections that can contribute to both. The planar diagrams are the first graphs that give additional information and are the subject of study in the presence of defect (boundaries) in the next section.

3.4 Boundary CFT and it's Holographic dual

The boundary CFT can be easily interpreted in its holographic dual. We consider an AdS_{d+1} whose boundary is realized by a AdS_d space. The space is given by the line element

$$ds^2 = \frac{dz_0^2 + d\vec{z}^2 + dz_\perp^2}{z_0^2}, \qquad z_\perp \geq = 0, \tag{3.8}$$

the AdS_d boundary is clearly realized at $z_\perp = 0$ and this space is called "half" Ads_{d+1} or simply $hAdS_{d+1}$. The effective action is then described by

$$S = \int_{AdS_{d+1}} \mathcal{L}_{\text{bulk}}[\varphi_i] + \int_{AdS_d} \mathcal{L}_{\text{boundary}}[\varphi_I] + \mathcal{L}_{\text{bulk-to-boundary}}[\varphi_i, \varphi_I]. \tag{3.9}$$

For the fields in the bulk of $hAdS_{d+1}$ we consider Neumann boundary conditions, $\partial_\perp \phi(z_0, \vec{z}, z_\perp)_{|_{z_\perp=0}} = 0$ and, for the boundary fields living on the AdS_d we don't have any condition. Propagators on the gravity side are realized by Green functions of the Klein-Gordon equation with their respective boundary conditions.

The first Witten diagram will compute the disconnected two-point function. We expect that this solution follows the solution of Example 2.2.1 which can be seen by computing the gravitational action with the Neumann boundary conditions and varying twice to get the 2−pt function by the AdS/CFT correspondence (Equation (3.4)), computation of this can be found in [5]. Thus we proceed to compute the relevant next-order diagrams for the two-point function in the defect theory shown in Figure 11.

The corresponding amplitudes of the Witten diagrams of Figure 11 are:

$$\begin{aligned}
W_{\text{Neum}}^{\text{contact}}(x,y) &= \int_{AdS_d} \frac{d^d w}{w_0^d} \widetilde{G}_{B\partial}^{\Delta_1}(w,x)\widetilde{G}_{B\partial}^{\Delta_2}(w,y), \\
W_{\text{Neum}}^{\text{bulk}}(x,y) &= \int_{AdS_d} \frac{d^d w}{w_0^d} \int_{hAdS_{d+1}^+} \frac{d^{d+1} z}{z_0^{d+1}} \widetilde{G}_{BB}^{\Delta}(w,z)\widetilde{G}_{B\partial}^{\Delta_1}(z,x)\widetilde{G}_{B\partial}^{\Delta_2}(z,y), \\
W_{\text{Neum}}^{\text{boundary}}(x,y) &= \int_{AdS_d} \frac{d^d w_1}{w_{10}^d} \frac{d^d w_2}{w_{20}^d} \widehat{\widetilde{G}}_{BB}^{\Delta}(w_1,w_2)\, \widetilde{G}_{B\partial}^{\Delta_1}(w_1,x)\, \widetilde{G}_{B\partial}^{\Delta_2}(w_2,y),
\end{aligned}$$

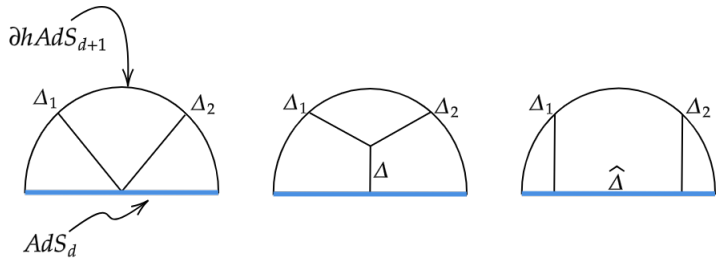

Figure 11: Witten diagrams: Contact, bulk, and, boundary at zeroth derivative order.

However, it is not the most convenient to work with the $hAdS_{d+1}$ propagators because of the nontrivial boundary condition. Instead, we can express the above Witten diagrams in terms only of the usual AdS propagators by embedding the defect in a full AdS_{d+1} as shown in Figure 12, in this setting the defect is called a interface. According to our rules for the Witten diagrams of Figure 12 take the amplitudes,

$$
\begin{aligned}
W^{\text{contact}}(x,y) &= \int_{AdS_d} \frac{d^d w}{w_0^d} G_{B\partial}^{\Delta_1}(w,x) G_{B\partial}^{\Delta_2}(w,y), \\
W^{\text{bulk}}(x,y) &= \int_{AdS_d} \frac{d^d w}{w_0^d} \int_{AdS_{d+1}} \frac{d^{d+1} z}{z_0^{d+1}} G_{BB}^{\Delta}(w,z) G_{B\partial}^{\Delta_1}(z,x) G_{B\partial}^{\Delta_2}(z,y), \\
W^{\text{boundary}}(x,y) &= \int_{AdS_d} \frac{d^d w_1}{w_{10}^d} \frac{d^d w_2}{w_{20}^d} G_{BB}^{\widehat{\Delta}}(w_1,w_2)\, G_{B\partial}^{\Delta_1}(w_1,x)\, G_{B\partial}^{\Delta_2}(w_2,y)\,.
\end{aligned}
$$

Now one can easily relate the W_{Neum} with W amplitudes by taking the transformations $x \to \bar{x} = (x,-r)$,

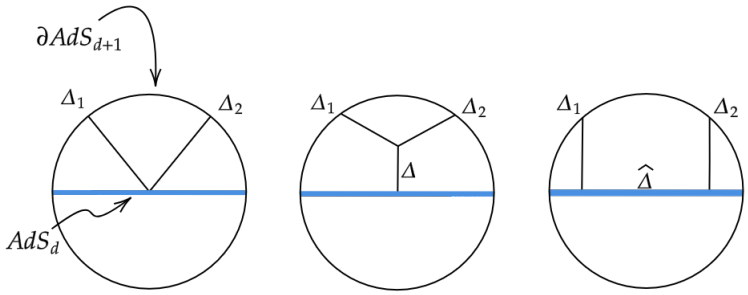

Figure 12: Witten diagrams: Contact, bulk, and boundary at zeroth derivative order Notice that the integration region of z has now been extended to the entire AdS_{d+1}.

using the symmetries of the propagators and, the fact that we are integrating over the interface, to give the relations

$$
\begin{aligned}
W^{\text{Contact}}_{\text{Neuman}}(x,y) &= 4W^{\text{Contact}}(x,y), \\
W^{\text{Bulk}}_{\text{Neuman}}(x,y) &= 2\big(W^{\text{Bulk}}(x,y) + W^{\text{Bulk}}(x,\bar{y})\big), \\
W^{\text{boundary}}_{\text{Neumann}}(x,y) &= 8W^{\text{boundary}}(x,y),
\end{aligned}
$$

where the 4 of the contact term comes from the possible combinations $x \to x, \bar{x}$ and $y \to y, \bar{y}$ we could have. Similar arguments follow for the second and third expressions. Furthermore, one can just solve the contact

diagram explicitly and find the others diagrams as the bulk Witten diagram and the contact Witten diagram satisfy:

$$\begin{aligned}\left(\frac{1}{2}\left(\mathrm{L}_1+\mathrm{L}_2\right)^2+\Delta(\Delta-d)\right)W^{\text{bulk}}(x,y)&\equiv\mathbb{EOM}_B[W^{\text{bulk}}(x,y)]=W^{\text{contact}}(x,y),\\ \left(\frac{1}{2}\left(\mathrm{L}_1+\widehat{\mathrm{L}}_2\right)^2+\Delta(\Delta-d)\right)W^{\text{bulk}}(x,y)&\equiv\overline{\mathbb{EOM}}_B[W^{\text{bulk}}(x,y)]=W^{\text{contact}}(x,y),\\ \left(\frac{1}{2}\hat{\mathrm{L}}_1^2+\hat{\Delta}(\hat{\Delta}-(d-1))\right)W^{\text{boundary}}(x,y)&\equiv\mathbb{EOM}_b[W^{\text{boundary}}(x,y)]=W^{\text{contact}}(x,y),\end{aligned}\tag{3.10}$$

where L_1 and L_2 are the generators of $SO(d,2)$ for operator 1 and 2 respectively, $\hat{L}_1$ is the generator of $SO(d-2,1)$ and $\widehat{\mathrm{L}}_2$ is the generator L_2 with $x\to\bar{x}$ coordinates. Notice that this is just the statement that the propagator of the exchange field is precisely the green function of the KG equation of the scalar field with dimension Δ.

Therefore, we can only compute the contact diagram and its conformal block expansions; details can be found in Appendix C. The result is

$$W^{\text{Contact}}(\xi)\equiv\frac{1}{y_\perp^{\Delta_2}x_\perp^{\Delta_1}}\mathcal{W}^{\text{Contact}}(\xi)=\frac{\pi^{\frac{d}{2}}(-1)^{1+\frac{3d}{2}}2^{1-\Delta_1-\Delta_2}\Gamma(\frac{\Delta_1+\Delta_2-(d-1)}{2})}{y_\perp^{\Delta_2}x_\perp^{\Delta_1}\Gamma(\frac{\Delta_1+\Delta_2+1}{2})}{}_2F_1\left(\Delta_1,\Delta_2;\frac{1}{2}\left(\Delta_1+\Delta_2+1\right);-\xi\right).$$

Performing the decomposition, the bulk conformal block contribution is made of double-trace operators with dimension $\Delta_1+\Delta_2+2N$,

$$\mathcal{W}^{\text{contact}}(\xi)=\sum_{N=0}^{\infty}a'_NG^B_{\Delta_1+\Delta_2+2N}(\xi),$$

where the conformal block is given by Equation (2.13),

$$G^B_\Delta(\xi)=\xi^{-\frac{\Delta_1+\Delta_2}{2}}\xi^{\frac{\Delta}{2}}{}_2F_1\left(\frac{\Delta+\Delta_1-\Delta_2}{2},\frac{\Delta+\Delta_2-\Delta_1}{2};\Delta-\frac{d}{2}+1;-\xi\right)$$

and the coefficients are

$$a'_N=\frac{\pi^{d/2}(-1)^N(\Delta_1)_N(\Delta_2)_N\left(\frac{\Delta_1+\Delta_2+1}{2}+N\right)_{-\frac{d}{2}}}{N!\left(-\frac{d}{2}+\Delta_1+\Delta_2+N\right)_N}.$$

Similarly, the boundary conformal block contribution is made of single-trace operators of dimension Δ_1+2N and Δ_2+2N decomposition gives:

$$\mathcal{W}^{\text{contact}}(\xi)=\sum_{N=0}^{\infty}a_NG^B_{\Delta_1+2N}(\xi)+b_NG^B_{\Delta_1+2N}(\xi),$$

where the conformal block is given by Equation (B.2),

$$G^b_{\widehat{\Delta}}(\xi)=\xi^{-\widehat{\Delta}_2}{}_2F_1\left(\widehat{\Delta},\widehat{\Delta}-\frac{d}{2}+1;2\widehat{\Delta}+2-d;-\xi^{-1}\right)$$

with coefficients

$$a_N=\frac{\pi^{d/2}2^{-2\Delta_1-4N-1}(\Delta_2)_{2N}\left(\Delta_1\right)_{2N}\left(-d-\Delta_2+2\right)_{\Delta_1}}{N!\left(\frac{3-d}{2}-\right)_{2N+\Delta_1}},\qquad b_N=\frac{\pi^{d/2}2^{-2\Delta_2-4N-1}(\Delta_1)_{2N}\left(\Delta_2\right)_{2N}\left(-d-\Delta_1+2\right)_{\Delta_2}}{N!\left(\frac{3-d}{2}\right)_{2N+\Delta_2}}.\tag{3.11}$$

Now, to see the bulk and boundary diagrams, we see how the operators involved in Equation (3.10) act on

the CBs [2] of single and double trace operators in the bulk and the boundary. We have

$$\begin{aligned}
\mathbb{EOM}_B[G^B_\Delta(\xi)] &= (\Delta(\Delta-d)-\Delta(\Delta-d))G^B_\Delta(\xi)=0\\
\mathbb{EOM}_B[G^b_{\Delta_1+n}(\xi)] &= \hat{\alpha}^{(1)}_n G^b_{\Delta_1+n-1}(\xi)+\hat{\beta}^{(1)}_n G^b_{\Delta_1+n}(\xi)+\hat{\gamma}^{(1)}_n G^b_{\Delta_1+n+1}(\xi),\\
\mathbb{EOM}_b[G^B_{\Delta_1+\Delta_2+2N}] &= \alpha_N G^B_{\Delta_1+\Delta_2+2N-2}+\beta_N G^B_{\Delta_1+\Delta_2+2N}+\gamma_N G^B_{\Delta_1+\Delta_2+2N+2}\\
\overline{\mathbb{EOM}}_B[G^b_{\Delta_1+n}(\xi)] &= \hat{\bar{\alpha}}^{(1)}_n G^b_{\Delta_1+n-1}(\xi)+\hat{\bar{\beta}}^{(1)}_n G^b_{\Delta_1+n}(\xi)+\hat{\bar{\gamma}}^{(1)}_n G^b_{\Delta_1+n+1}(\xi),\\
\overline{\mathbb{EOM}}_B[G^B_{\Delta_1+\Delta_2+2N}(\xi)] &= \bar{\alpha}_N G^B_{\Delta_1+\Delta_2+2N-2}+\bar{\beta}_N G^B_{\Delta_1+\Delta_2+2N}+\bar{\gamma}_N G^B_{\Delta_1+\Delta_2+2N+2},
\end{aligned} \tag{3.12}$$

where all the coefficients are defined in Section 3.4-3.6 of [2]. Applying (3.10) and (3.12) to the contact bulk and boundary channel we can find the decomposition coefficients of the tower operators of the remaining diagrams. The only coefficient that remains to be computed is the single CB decomposition of each channel which can not be retrieved from this as they have vanishing eigenvalue in the equation (3.10), see [2] for a derivation of those. The upshot is:

$$\begin{aligned}
\mathcal{W}^{\text{Bulk}}(\xi) &= A^B g^B_\Delta(\xi)+\sum_N A^B_N G^B_{\Delta_1+\Delta_2+2N}(\xi)=\sum_n \hat{A}^{B,(1)}_n G^b_{\Delta_1+n}(\xi)+\sum_n \hat{A}^{B,(2)}_n G^b_{\Delta_2+n}(\xi),\\
\mathcal{W}^{\text{Bdry}}(\xi) &= A^b G^b_{\hat{\Delta}}(\xi)+\sum_N A^b_N G^b_{\Delta_1+2N}(\xi)+B^b_N G^b_{\Delta_2+2N}(\xi)=\sum_N A^b_n G^B_{\Delta_1+\Delta_2+2N}(\xi),\\
\overline{\mathcal{W}}^{\text{Bulk}}(\xi) &= \sum_n \hat{\bar{A}}^{B,(1)}_n G^b_{\Delta_1+n}(\xi)+\sum_n \hat{\bar{A}}^{B,(2)}_n G^b_{\Delta_2+n}(\xi)=\sum_N \bar{A}^B_N G^B_{\Delta_1+\Delta_2+2N}(\xi).
\end{aligned}$$

Which finally allows to write our $hAdS_{d+1}$ amplitudes of Figure 12 as:

$$\mathcal{W}^{\text{Bulk}}_{\text{Neumann}}(\xi)=2\left(A^B g^B_\Delta(\xi)+\sum_N\left(A^B_N+\bar{A}^B_N\right)G^B_{\Delta_1+\Delta_2+2N}(\xi)\right) \tag{3.13}$$

$$=2\sum_{n\in 2\mathbb{N}+1}\left(\left(\hat{\bar{A}}^{B,(1)}_n+\hat{A}^{B,(1)}_n\right)G^b_{\Delta_1+n}(\xi)+\left(\hat{A}^{B,(2)}_n+\hat{\bar{A}}^{B,(2)}_n\right)G^b_{\Delta_2+n}(\xi)\right), \tag{3.14}$$

$$\mathcal{W}^{\text{Boundary}}_{\text{Neumann}}(\xi)=8\left(A^b G^b_{\hat{\Delta}}(\xi)+\sum_N A^b_N G^b_{\Delta_1+2N}(\xi)+B^b_N G^b_{\Delta_2+2N}(\xi)\right)=8\left(\sum_N A^B_n G^B_{\Delta_1+\Delta_2+2N}(\xi)\right) \tag{3.15}$$

where we used the fact that $\hat{A}^{B,(2)}_{2n}=-\hat{\bar{A}}^{B,(2)}_{2n}$ and $\hat{\bar{A}}^{B,(1)}_n=-\hat{A}^{B,(1)}_n$. We, therefore, find that all the single-trace boundary conformal blocks with conformal dimensions Δ_i+2n+1 are projected out. This is precisely what we expected for the Neumann boundary condition.

Similarly, as for the case of the $4-pt$ functions in AdS_{d+1}, the contact term is compatible with the crossing symmetry while the bulk and boundary are not individually cross-symmetric. This is as expected as we saw that the decomposition of double trace operators is entirely determined by single trace operators being exchanged. The contributions of the single blocks Δ and $\hat{\Delta}$, however, can not be determined but instead we needed to perform the integrals, this information depends entirely on the interaction of the bulk fields. Higher order contributions are needed to full fill crossing symmetry and the sum of all the diagrams will be manifestly crossing symmetric.

[2] More precisely, the CBs form a basis in which the operators $\mathbb{EOM}$ are block diagonal

4 Future Work and Conclusions

In this work, we approached boundary CFTs from the holographic side. The main beneficial tool is the computation of the contact term, which already is compatible with crossing symmetry, to compute the bulk and boundary channels. The analysis follows closely from the $4-pt$ function of holographic CFTs without the presence of the defect. It seems interesting to explore that the key ingredients of the defect-crossing symmetry are 1) The already defect-crossing symmetric conformal block expansion of the contact diagram and, 2) Few single trace operators decomposition of both diagrams. Mainly, the bulk and boundary exchanged contributions. Our intuition on the gravity side says that the extra information derived from those are just dynamics of interaction in the bulk that do not contribute to more information in the crossing equation.

This approach greatly reduces the number of computations to describe the defect crossing equation but still, a systematic procedure to extract the CB decomposition of crossed channels is needed, as most of the coefficients are determined and only a small specific number of CB decompositions must be performed explicitly. Performing these computations in the Mellin formalism will be extremely efficient to extract this information as we already know the prescription of which CBs are needed.

Notice that the operators $\mathbb{EOM}[\mathcal{W}^{Bulk/Boundary}] = \mathcal{W}^{\text{Contact}}$ of equations (3.10) define a differential equation on the CB expansion. The information that is not fixed by this in the diagrams, i.e. the homogenous equation, is precisely the exchange diagrams of the operators. We conclude that the Witten diagrams constitute the OPE data given that the homogenous part is precisely the exchanged bulk or boundary field that corresponds to the dual CFT of the according dimension. An observation was made in [16] but made precise in this context. Finally, we consider there are several directions one can take here:

- How important are the C and $\hat{C}$ coefficients? It seems that any excitation of the defect can be reproduced out of bulk fields near the defect so it seems that one of them is not so important.
- It would be interesting to explore higher-order diagrams. In particular, loops already present anomalous dimension contributions and they will contribute to double trace operators of the crossing equation.
- Even though we didn't discuss the proof of the "cutting rule" it seems straightforward to implement those methods of [17], using Geodesic Witten diagrams, to find the conformal block decomposition rule analog for the boundary CFT.

Appendix

A Bulk-Defect two-point Functions in dCFTs

We saw in Section 2.1 that the building blocks to build transversal quantities is C^{IJ}. As argued before, we can write bulk-only correlations only in terms of the mixed C_{AI} since the following equalities hold:

$$\begin{aligned} C_{AB}Q^A R^B &= \frac{P\bullet R}{P\circ G}C_{AI}Q^A G^I - \frac{P\bullet Q}{P\circ G}C_{AI}R^A G^I, \\ C^{IJ}Q^I R^J &= \frac{P\circ Q}{P\bullet G}C_{AI}G^A R^I - \frac{P\circ R}{P\bullet G}C_{AI}G^A Q^I. \end{aligned} \tag{A.1}$$

Also,

$$C^{AI}C_{BI}C^{BJ} = \frac{1}{2}\left(C^{BI}C_{BI}\right)C^{AJ}$$

so that we don't have to concatenate more than two of this building blocks. We compute a general bulk to defect 2pt functions,

$$\langle O_{\Delta,J}(P_1,Z_1)\hat{O}_{\hat{\Delta},j,s}(P_2,Z_2,W_2)\rangle.$$

For this quantity, the only Lorentz invariant transverse quantity in which Z_2 can appear is $C_2^{AB} = P_2^A Z_2^B - P_2^B Z_2^A$ which is our building block together with C_1^{AI}. We can contract C_2^{AB} with either Z_1 or P_1 but other contractions give gauge redundant fields since $P^2 = Z^2 = P\cdot Z = 0$. For terms contracted with Z_1, they can further only be written as a contraction between C_2^{AB} and C_1^{AI}. Therefore, following the notation of [1] ,the term that contains Z_2 is always given by

$$Q^0_{BD} = \frac{C_1^{AB}C_{2,AB}}{2P_1\bullet P_2} = \frac{P_1\bullet P_2 Z_1\bullet Z_2 - P_2\bullet Z_1 Z_2\bullet P_1}{P_1\bullet P_2}.$$

We conclude that the most general tensor structure is given by the product of Q^0_{BD} with other factors built out of at most two copies of C_1^{AI}, contracted with P_1, P_2 and W_2. The independent ones among these remaining structures are

$$\begin{aligned} Q^1_{BD} &= \frac{P_1\circ W_2}{(P_1\circ P_1)^{1/2}}, & Q^3_{BD} &= \frac{W_2\circ Z_1 P_1\circ P_1 - P_1\circ W_2 P_1\circ Z_1}{P_1\circ P_1}, \\ Q^2_{BD} &= \frac{P_1\circ Z_1 P_1\bullet P_2 - P_2\bullet Z_1 P_1\circ P_1}{(P_1\circ P_1)^{1/2}(P_1\bullet P_2)}, & Q^4_{BD} &= \left(\frac{C_1^{AI}C_{1AI}}{2P_1\circ P_1}\right), \end{aligned}$$

Thus, a generic bulk-to-defect two-point function is given by

$$\left\langle O_{\Delta,J}(P_1,Z_1)\,\widehat{O}_{\widehat{\Delta},j,s}(P_2,Z_2,W_2)\right\rangle = \left(Q^0_{BD}\right)^j \sum_{\{n_i\}} b_{n_1\ldots n_4}\frac{\prod_{k=1}^4\left(Q^k_{BD}\right)^{n_k}}{(-2P_1\bullet P_2)^{\widehat{\Delta}}\,(P_1\circ P_1)^{\frac{\Delta-\widehat{\Delta}}{2}}},$$

where the sum runs over integers n_i satisfying the condition $n_1+n_3 = s$, so that W_1 scales as s and $n_2+n_3+2n_4 = J-j$ so that Z_1 scale as J.

B Bulk and defect conformal blocks

B.1 Computation of the Conformal Blocks

To impose the constraints on the CFT data with Equation 1.12 we need to find the Conformal Blocks (CBs). One trick to find them is to apply the Casimir operator of $SO(d+1,1)$ ingeniously. Inserting a resolution of the identity, $P_{\mathcal{O}} = \sum_{\alpha,\beta\in\text{multiplet}} N_{\alpha\beta}\,|\alpha\rangle\,\langle\beta|$, given by primary projectors whose scaling dimension is Δ, I, we can isolate $G_{\Delta,I}$ giving:

$$\langle 0|\,\mathcal{O}_1\mathcal{O}_2 P_{\mathcal{O}}\mathcal{O}_3\mathcal{O}_4\,|0\rangle = \frac{1}{|x_{12}|^{2\Delta}|x_{34}|^{2\Delta}} G_{\Delta,I}(u,v).$$

Now, we use the quadratic Casimir for the $SO(d+1,1)$ group,

$$C_2 = \frac{1}{2}M^{\mu\nu}M_{\mu\nu} = \frac{1}{2}M^{ij}M_{ij} - D^2 + \frac{1}{2}\{P_i, K^i\} = \frac{1}{2}M^{ij}M_{ij} - D(D - i(d)) - P_iK^i$$

where we see that the primary state satisfies $C_2\,|\mathcal{O}\rangle = (-\Delta(\Delta-d) - \ell(\ell+d-2))\,|\mathcal{O}\rangle \equiv \lambda_{\Delta,\ell}\,|\mathcal{O}\rangle$. Therefore, we insert the Casimir applying to the state $\mathcal{O}_3$ which can be seen as an operator on x_3 and x_4 variables or as an operator on the states. This gives

$$\langle 0|\,\mathcal{O}_1\mathcal{O}_2|P_{\mathcal{O}}|C_2\mathcal{O}_3\mathcal{O}_4\,|0\rangle = \lambda_{\Delta,\ell}\frac{f^2_{\mathcal{O}\mathcal{O}\mathcal{O}}}{|x_{12}|^{2\Delta}|x_{34}|^{2\Delta}} G_{\Delta,\ell}, = D_{x_3,x_4}\left(\frac{f^2_{\mathcal{O}\mathcal{O}\mathcal{O}}}{|x_{12}|^{2\Delta}|x_{34}|^{2\Delta}} G_{\Delta,\ell}(u,v)\right)$$

meaning that the conformal blocks are eigenstates of the Casimir operator. One can explicitly have

$$D = \left(\left(2z^2(z-1)\partial_z^2 + 2z^2\partial_z\right) + c.c\right) + 2(d-2)\frac{z\bar{z}}{z-\bar{z}}((z-1)\partial_z - c.c.)$$

where $z = x_3 + ix_4$. We solve this equation to find the form of the conformal blocks.

B.2 Defect conformal blocks

In the light cone, in the presence of a defect, the two-point function is

$$\langle \mathcal{O}_1(P_1)\mathcal{O}_2(P_2)\rangle = \frac{f(\xi,\phi)}{(P_1\circ P_1)^{\Delta_1/2}(P_2\circ P_2)^{\Delta_2/2}}$$

where f is any function of the invariants ξ, ϕ. The Casimir equation for defect channel splits into each of the direct product Casimrs $S^2 = \frac{1}{2}(J_{IJ})^2$ and $L^2 = \frac{1}{2}(J_{AB})^2$, therefore,

$$f(\xi,\phi) = \xi^{-(\Delta_1+\Delta_2)/2}\sum_k c_{12k}a_k f_{\Delta_k,J}(\xi,\phi) = \sum_{\widehat{\mathcal{O}}} b_{1\widehat{\mathcal{O}}}b_{2\widehat{\mathcal{O}}}\widehat{f}_{\widehat{\Delta},0,s}(\xi,\phi).$$

together with the constrain

$$\left(D_{L^2} + \widehat{\lambda}_{\widehat{\Delta},0}\right)\frac{\widehat{f}_{\widehat{\Delta},0,s}}{(P_1\circ P_1)^{\frac{\Delta_1}{2}}(P_2\circ P_2)^{\frac{\Delta_2}{2}}} = 0, \quad \left(D_{S^2} + \widehat{\lambda}_{0,s}\right)\frac{\widehat{f}_{\widehat{\Delta},0,s}}{(P_1\circ P_1)^{\frac{\Delta_1}{2}}(P_2\circ P_2)^{\frac{\Delta_2}{2}}} = 0 \tag{B.1}$$

where

$$D_{S^2} \equiv 4\cos\phi(1-\cos\phi)\frac{\partial^2}{\partial\cos\phi^2} + 2(1-q\cos\phi)\frac{\partial}{\partial\cos\phi} + \widehat{C}_{0,s},$$
$$D_{L^2} \equiv \left(4-\chi^2\right)\frac{\partial^2}{\partial\chi^2} - (p+1)\chi\frac{\partial}{\partial\chi} + \widehat{C}_{\Delta,0}$$

and we used

$$\chi = -\frac{2P_1\bullet P_2}{(P_1\circ P_1)^{\frac{1}{2}}(P_2\circ P_2)^{\frac{1}{2}}}, \qquad \xi = -\frac{2P_1\cdot P_2}{(P_1\circ P_1)^{\frac{1}{2}}(P_2\circ P_2)^{\frac{1}{2}}}, \qquad \cos\phi = \frac{P_1\circ P_2}{(P_1\circ P_1)^{\frac{1}{2}}(P_2\circ P_2)^{\frac{1}{2}}}.$$

We solve this system of equations to find the defect conformal blocks which for a codimension 1 flat defect we call the boundary conformal blocks. This expression however can be computed explicitly from the OPE, the boundary conformal block is then given by

$$G_\Delta^{\text{boundary}}(\xi_1) = \frac{1}{\xi_1^{\hat{\Delta}}}{}_2F_1\left(\hat{\Delta}, 1-\frac{d}{2}+\hat{\Delta}, 2-d+2\hat{\Delta}, -\frac{1}{\xi_1}\right), \tag{B.2}$$

the computation can be found in [15].

C Computation of the contact diagrams and conformal block expansion

Let us proceed with the computation of the contact term. **Bulk-to-Bulk propagator on** AdS_{d+1}

$$(\Box_{d+1} - \underbrace{\Delta(\Delta-d)}_{M^2})G_{BB}^\Delta(z,w) = \delta^{d+1}(z,w). \tag{C.1}$$

Since we proved that we only need the propagators on AdS_{d+1} to write the diagrams, solving the differential equations gives:

$$G_{BB}^\Delta(w,z) = \frac{\Gamma(\Delta)}{2\pi^{\frac{d}{2}}\Gamma\left(\Delta-\frac{d}{2}+1\right)}u^{-\Delta_2}{}_2F_1\left(\Delta, \frac{2\Delta-d+1}{2}, 2\Delta-d+1, -\frac{4}{u}\right),$$
$$G_{BB}^{\widehat{\Delta}}(w,z) = \frac{\Gamma(\widehat{\Delta})}{2\pi^{\frac{d-1}{2}}\Gamma\left(\widehat{\Delta}-\frac{d-1}{2}+1\right)}u^{-\widehat{\Delta}_2}{}_2F_1\left(\widehat{\Delta}, \frac{2\widehat{\Delta}-d+2}{2}, 2\widehat{\Delta}-d+2, -\frac{4}{u}\right),$$
$$G_{B\partial}^\Delta(z,x) = \left(\frac{z_0}{z_0^2+(\vec{z}-\vec{x})^2+(z_\perp-x_\perp)^2}\right)^\Delta,$$

where we have defined

$$u = \frac{(\vec{w}-\vec{z})^2+(w_\perp-z_\perp)^2+(w_0-z_0)^2}{w_0z_0}.$$

C.1 Contact term Witten diagram amplitude

We are going to compute

$$W^{\text{contact}}(x,y) = \int_{AdS_d} \frac{d^d w}{w_0^d} G_{B\partial}^{\Delta_1}(w,x) G_{B\partial}^{\Delta_2}(w,y)$$

and show the conformal block expansion.

$$\begin{aligned} W^{\text{contact}}(x,y) &= \int_{AdS_d} \frac{d^d w}{w_0^d} w_0^{\Delta_1+\Delta_2} \frac{1}{\left(w_0^2 + (\vec{w}-\vec{x})^2 + (w_\perp - x_\perp)^2\right)^\Delta} \frac{1}{\left(w_0^2 + (\vec{w}-\vec{x})^2 + (w_\perp - x_\perp)^2\right)^\Delta} \\ &= \int_{AdS_d} \frac{d^d w}{w_0^d} w_0^{\Delta_1+\Delta_2} \frac{\Gamma(\Delta_1+\Delta_2)}{\Gamma(\Delta_1)\Gamma(\Delta_2)} \int_0^1 d\alpha \frac{\alpha^{\Delta_1-1}(1-\alpha)^{\Delta_2-1}}{\left[(\vec{w}-\alpha\vec{x})^2 + w_0^2 + \Delta(\alpha)\right]^{\Delta_1+\Delta_2}} \end{aligned}$$

where we used the Feynman parametrization in the second equality and the definition $\Delta(\alpha) = \alpha x_\perp^2 + (1-\alpha) y_\perp^2 + \alpha(1-\alpha)\vec{x}^2$. Setting $p = \frac{\Delta_1+\Delta_2-d}{2}$, $n = \Delta_1+\Delta_2$ and using the Formula (D.2) on the one dimensional integral over w_0 and performing the translation in the bulk $\vec{w} - \alpha\vec{x} \to \vec{w}$,

$$W^{\text{contact}}(x,y) = \int_0^1 d\alpha \frac{\alpha^{\Delta_1-1}(1-\alpha)^{\Delta_2-1}}{\Gamma(\Delta_1)\Gamma(\Delta_2)} \int d^d\vec{w} \frac{(2\pi) i (-1)^{\frac{1}{2}+\Delta_1+\Delta_2+d} \Gamma(\frac{\Delta_1+\Delta_2-d+1}{2}) \Gamma(\frac{\Delta_1+\Delta_2+d-1}{2})}{(4\pi)^{\frac{1}{2}} \Gamma(\frac{1}{2}) \left[\vec{w}^2 + \Delta(\alpha)\right]^{\frac{\Delta_1+\Delta_2+d-1}{2}}}$$

Again, performing in the remaining dimensions the Formula (D.2) with $p = 0$, $n = \frac{\Delta_1+\Delta_2+d-1}{2}$

$$\begin{aligned} &= \int_0^1 d\alpha \frac{\alpha^{\Delta_1-1}(1-\alpha)^{\Delta_2-1}}{\Gamma(\Delta_1)\Gamma(\Delta_2)\Gamma(\frac{1}{2})} \pi^{d/2} (-1)^{1+3d/2} \Gamma(\frac{\Delta_1+\Delta_2-d+1}{2}) \Gamma(\frac{\Delta_1+\Delta_2}{2}) \frac{1}{\Delta(\alpha)^{\frac{\Delta_1+\Delta_2}{2}}} \\ &\equiv C \int_0^1 d\alpha \frac{\alpha^{\Delta_1-1}(1-\alpha)^{\Delta_2-1}}{\left[\alpha x_\perp^2 + (1-\alpha) y_\perp^2 + \alpha(1-\alpha)\vec{x}^2\right]^{\frac{\Delta_1+\Delta_2}{2}}} \end{aligned}$$

where $C = \frac{\pi^{d/2}(-1)^{1+3d/2}\Gamma(\frac{\Delta_1+\Delta_2-d+1}{2})\Gamma(\frac{\Delta_1+\Delta_2}{2})}{\Gamma(\Delta_1)\Gamma(\Delta_2)\Gamma(\frac{1}{2})}$. We can set $\vec{x} \to 0$ and later restore the ξ dependence. To solve this integral, we factorize $y_\perp^{\Delta_1+\Delta_2}$ out of the denominator, giving

$$\begin{aligned} &= \frac{C}{y_\perp^{\Delta_1+\Delta_2}} \int_0^1 d\alpha \alpha^{\Delta_1-1}(1-\alpha)^{\Delta_2-1} \left[1 - \alpha\left(1 - \left(\frac{x_\perp}{y_\perp}\right)^2\right)\right]^{-\frac{\Delta_1+\Delta_2}{2}} \\ &= \frac{C}{x_\perp^{\Delta_1} y_\perp^{\Delta_2}} \zeta^{\Delta_1} \frac{\Gamma(\Delta_1)\Gamma(\Delta_2)}{\Gamma(\Delta_1+\Delta_2)} {}_2F_1\left(\frac{\Delta_1+\Delta_2}{2}, \Delta_1, \Delta_1+\Delta_2; 1 - \frac{x_\perp^2}{y_\perp^2}\right) \end{aligned}$$

were we read from the integral description of the hypergeometric function, ${}_2F_1(a,b,c;z)$ that $a = \frac{\Delta_1+\Delta_2}{2}$, $b = \Delta_1$, $c = \Delta_1+\Delta_2$ and $z = 1 - \frac{x_\perp^2}{y_\perp^2}$ and we used $\zeta^2 = \left(\frac{x_\perp}{y_\perp}\right)^2$. Finally, to restore back the ξ dependence, recall $\xi = \frac{(\vec{x}-\vec{y})^2 + (x_\perp - y_\perp^2)^2}{4 x_\perp y_\perp}$, in our limit,

$$\xi = \frac{1}{4}\left(\frac{x_\perp}{y_\perp} - 2 + \frac{y_\perp}{x_\perp}\right) = \frac{1}{4}\left(\zeta - 2 + \zeta^{-1}\right).$$

Solving for ζ, we find $\zeta = 1 + 2\xi + 2\sqrt{\xi(1+\xi)}$ where we only took the positive root. Putting all together,

$$W^{\text{Contact}}(x,y) = \frac{\pi^{\frac{d-1}{2}}(-1)^{1+\frac{3d}{2}}\Gamma(\frac{\Delta_1+\Delta_2-(d-1)}{2})\Gamma(\frac{\Delta_1+\Delta_2}{2})}{\Gamma(\Delta_1+\Delta_2) y_\perp^{\Delta_2} x_\perp^{\Delta_1}} \zeta^{\Delta_1} {}_2F_1\left(\frac{\Delta_1+\Delta_2}{2}, \Delta_1, \Delta_1+\Delta_2; 1-\zeta^2\right) \tag{C.2}$$

One can further simplify this result to get into the more familiar form of [2],

$$
\begin{aligned}
{}_2F_1(\Delta_1,\Delta_2,\frac{\Delta_1+\Delta_2+1}{2};\frac{1-\sqrt{1-x}}{2}) &= {}_2F_1\left(\frac{\Delta_1}{2},\frac{\Delta_1+\Delta_2-\Delta_1}{2},\frac{\Delta_1+\Delta_2+1}{2},\underbrace{\frac{z^2}{4(z-1)}}_{x}\right)\\
&= (1-z)^{\frac{\Delta_1}{2}}{}_2F_1(\Delta_1,\frac{\Delta_1+\Delta_2}{2},\Delta_1+\Delta_2,z)\\
&= (1-z)^{\frac{\Delta_1}{2}}{}_2F_1(\frac{\Delta_1+\Delta_2}{2},\Delta_1,\Delta_1+\Delta_2,\underbrace{z}_{1-\zeta^2})
\end{aligned}
$$

where we used the identities:

$$
\begin{aligned}
{}_2F_1(a,b;2b;z) &= {}_2F_1(b,a;2b;z)\\
{}_2F_1(a,b;2b;z) &= (1-z)^{-\frac{a}{2}}{}_2F_1\left(\frac{a}{2},b-\frac{a}{2};b+\frac{1}{2};\frac{z^2}{4z-4}\right),\\
{}_2F_1\left(a,b;a+b+\frac{1}{2};z\right) &= {}_2F_1\left(2a,2b;a+b+\frac{1}{2};\frac{1-\sqrt{1-z}}{2}\right).
\end{aligned}
$$

Plugging in the ζ definition in terms of ξ,

$$
1-\zeta^2 \to \frac{(1-\zeta^2)^2}{4(1-\zeta^2-1)} \to \frac{1-\sqrt{1-x}}{2} = -\xi
$$

therefore we have

$$
\begin{aligned}
W^{\text{Contact}}(x,y) &= \frac{\pi^{\frac{d-1}{2}}(-1)^{1+\frac{3d}{2}}\Gamma(\frac{\Delta_1+\Delta_2-(d-1)}{2})\Gamma(\frac{\Delta_1+\Delta_2}{2})}{y_\perp^{\Delta_2}x_\perp^{\Delta_1}\Gamma(\Delta_1+\Delta_2)}{}_2F_1\left(\Delta_1,\Delta_2;\frac{1}{2}\left(\Delta_1+\Delta_2+1\right);-\xi\right)\\
&= \frac{\pi^{\frac{d}{2}}(-1)^{1+\frac{3d}{2}}2^{1-\Delta_1-\Delta_2}\Gamma(\frac{\Delta_1+\Delta_2-(d-1)}{2})}{y_\perp^{\Delta_2}x_\perp^{\Delta_1}\Gamma(\frac{\Delta_1+\Delta_2+1}{2})}{}_2F_1\left(\Delta_1,\Delta_2;\frac{1}{2}\left(\Delta_1+\Delta_2+1\right);-\xi\right)
\end{aligned}
$$

where we used the Legendre duplication formula: $\Gamma(z)\Gamma\left(z+\frac{1}{2}\right) = 2^{1-2z}\sqrt{\pi}\,\Gamma(2z)$.

C.2 Bulk conformal block decomposition of the contact diagram

The bulk conformal block decomposition is

$$
\mathcal{W}^{\text{contact}}(\xi) = \sum_{N=0}^{\infty} a_N g^B_{\Delta_1+\Delta_2+2N}(\xi)
$$

where

$$
g^B_\Delta(\xi) = \xi^{-\frac{\Delta_1+\Delta_2}{2}}\xi^{\frac{\Delta}{2}}{}_2F_1\left(\frac{\Delta+\Delta_1-\Delta_2}{2},\frac{\Delta+\Delta_2-\Delta_1}{2};\Delta-\frac{d}{2}+1;-\xi\right),
$$

to find the coefficients lets expand the $\mathcal{W}^{\text{contact}}$ and reorganize in terms of the conformal blocks,

$$\begin{aligned}\pi^{d/2}\left(\frac{\Delta_1+\Delta_2+1}{2}\right)_{-\frac{d}{2}}{}_2F_1\left(\Delta_1,\Delta_2,\frac{\Delta_1+\Delta_2+1}{2},-\xi\right)&\\ =\sum_N a_N\xi^N{}_2F_1\left(\Delta_1+N,\Delta_2+N,\Delta_1+\Delta_2+2N-\frac{d}{2}+1,-\xi\right)&\\ =\sum_N a_N\xi^N\sum_{l=0}^{\infty}\frac{(\Delta_1+N)_l(\Delta_2+N)_l}{(\Delta_1+\Delta_2+2N-\frac{d}{2}+1)_l}\frac{(-\xi)^l}{l!}&\end{aligned}$$

set $a_N=\pi^{\frac{d}{2}}(-1)^N\left(\frac{\Delta_1+\Delta_2+1}{2}\right)_{-\frac{d}{2}}(\Delta_1)_N(\Delta_2)_N a'_N$, then we have the constrain

$$\begin{aligned}{}_2F_1\left(\Delta_1,\Delta_2,\frac{\Delta_1+\Delta_2+1}{2},-\xi\right)&=\sum_N a_N\xi^N{}_2F_1\left(\Delta_1+N,\Delta_2+N,\Delta_1+\Delta_2+2N-\frac{d}{2}+1,-\xi\right)\\ &=\sum_N^{\infty}\sum_{l=0}^{N}a'_{N-l}\frac{(-\xi)^N}{l!}\frac{(\Delta_1)_N(\Delta_2)_N}{(\Delta_1+\Delta_2+2(N-l)-\frac{d}{2}+1)_l}\\ &=\sum_N^{\infty}\frac{(\Delta_1)_N(\Delta_2)_N}{\left(\frac{\Delta_1+\Delta_2+1}{2}\right)_N}\frac{(-\xi)^N}{N!}\left[\sum_l^N a'_{N-l}\frac{N!}{l!}\frac{\left(\frac{\Delta_1+\Delta_2+1}{2}\right)_N}{(\Delta_1+\Delta_2+2(N-l)-\frac{d}{2}+1)_l}\right]\end{aligned}$$

From the relation $(\frac{a}{2})_N 2^N=\frac{(a+2(N-1))!!}{(a-1)!!}$ we can set $a'_{N-l}=\frac{1}{(N-l)!}\frac{(\Delta_1+\Delta_2+2(N-l)-\frac{d}{2}+1)_l}{\left(\frac{\Delta_1+\Delta_2+1}{2}\right)_N}$ giving the square bracket the usual binomial expansion of 2^N and therefore completing the equality. Plugging back this definition, a_N can be simplified to

$$a_N=\frac{\pi^{d/2}(-1)^N(\Delta_1)_N(\Delta_2)_N\left(\frac{\Delta_1+\Delta_2+1}{2}+N\right)_{-\frac{d}{2}}}{N!\left(-\frac{d}{2}+\Delta_1+\Delta_2+N\right)_N}$$

giving the bulk decomposition of the contact diagram,

$$\mathcal{W}^{\text{contact}}(\xi)=\sum_{N=0}^{\infty}a_N g^B_{\Delta_1+\Delta_2+2N}(\xi).$$

C.3 Boundary conformal block decomposition of the contact diagram

Now, we proceed to the other side of the picture with the boundary conformal block expansion. This expansion should depend symmetrically on Δ_1 and Δ_2 giving the so-called "towers of single trace operators" of dimension Δ_1+n and Δ_2+n. To do so we transform into Mellin space where the boundary conformal blocks are the ones derived in Appendix B.2,

$$g^b_{\widehat{\Delta}}(\xi)=\xi^{-\widehat{\Delta}_2}F_1\left(\widehat{\Delta},\widehat{\Delta}-\frac{d}{2}+1;2\widehat{\Delta}+2-d;-\xi^{-1}\right).$$

The contact amplitude in Mellin space reads:

$$\frac{\pi^{d/2}\left(\frac{1}{2}(\Delta_1+\Delta_2+1)\right)_{-h}\left(\Gamma\left(\frac{1}{2}(\Delta_1+\Delta_2+1)\right)\Gamma(s)\Gamma(\Delta_1-s)\Gamma(\Delta_2-s)\right)}{\Gamma(\Delta_1)\Gamma(\Delta_2)\Gamma\left(\frac{1}{2}(-2s+\Delta_1+\Delta_2+1)\right)},$$

while the boundary conformal blocks give:

$$\frac{\Gamma(s)2^{2\Delta_1-2h+4N+1}\Gamma(-h+s+1)\Gamma\left(-h+2N+\Delta_1+\frac{3}{2}\right)\Gamma\left(2N-s+\Delta_1\right)}{\sqrt{\pi}\Gamma\left(2N+\Delta_1\right)\Gamma\left(-2h+2N+s+\Delta_1+2\right)}.$$

Doing the decomposition and, setting

$$a_{\mathrm{N}} \coloneqq a'_N\left(\frac{1}{2}\left(\Delta_1+\Delta_2+1\right)\right)_{-h}\frac{\sqrt{\pi}\left(\pi^{d/2}\Gamma\left(\frac{1}{2}\left(\Delta_1+\Delta_2+1\right)\right)\right)\Gamma\left(2N+\Delta_1\right)}{\left(\Gamma\left(\Delta_1\right)\Gamma\left(\Delta_2\right)\right)\left(4^{\Delta_1}2^{-2h+4N+1}\Gamma\left(-h+2N+\Delta_1+\frac{3}{2}\right)\right)}$$
$$b_{\mathrm{N}} \coloneqq \left(b'_N \leftrightarrow a'_N, \Delta_1 \leftrightarrow \Delta_2\right)$$

we need a'_N and b'_N such that

$$\Gamma(-h+s+1)\sum_{N=0}^{\infty}\frac{a'_N\Gamma\left(2N-s+\Delta_1\right)\Gamma\left(-2h+2N+s+\Delta_2+2\right)}{\Gamma\left(-2h+2N+s+\Delta_1+2\right)\Gamma\left(-2h+2N+s+\Delta_2+2\right)}+\left(b'_N \leftrightarrow a'_N, \Delta_1 \leftrightarrow \Delta_2\right)$$
$$=\frac{\Gamma\left(\Delta_1-s\right)\Gamma\left(\Delta_2-s\right)}{\Gamma\left(\frac{1}{2}\left(-2s+\Delta_1+\Delta_2+1\right)\right)}.$$

Using the well known identity of the Hypergeometric function, ${}_2F_1(a,b,c,1)=\frac{\Gamma(a)\Gamma(b)\Gamma(c-a-b)}{\Gamma(c-a)\Gamma(c-b)}$ and setting $a'_N \coloneqq \Gamma(\alpha+2N)a/N!$, $b'_N \coloneqq \Gamma(\beta+2N)b/N!$,

$$\frac{\Gamma\left(-h+s+\frac{3}{2}\right)}{\Gamma\left(-s+\frac{\Delta_1}{2}+\frac{\Delta_2}{2}+\frac{1}{2}\right)}=\frac{2^{-\alpha}a\left(\Gamma(\alpha)\Gamma\left(-h+s-\frac{\alpha}{2}+1\right)\right)\Gamma\left(-h+s-\frac{\alpha}{2}+\frac{3}{2}\right)}{\Gamma\left(\Delta_2-s\right)\Gamma\left(-2h+s-\alpha+\Delta_1+2\right)}+\left(b\leftrightarrow a,\Delta_1\leftrightarrow\Delta_2,\beta\leftrightarrow\alpha\right)$$

since this holds for any s, taking the 0 term in expansion on s centered at 0 gives the solution with

$$a=\frac{2^{\alpha-1}\Gamma\left(\frac{3}{2}-h\right)}{\frac{\Gamma\left(\frac{1}{2}(\Delta_1+\Delta_2+1)\right)\left(\Gamma(\alpha)\Gamma\left(-h-\frac{\alpha}{2}+1\right)\Gamma\left(-h-\frac{\alpha}{2}+\frac{3}{2}\right)\right)}{\Gamma(\Delta_2)\Gamma(-2h-\alpha+\Delta_1+2)}},\quad b=\frac{2^{\beta-1}\Gamma\left(\frac{3}{2}-h\right)}{\frac{\Gamma\left(\frac{1}{2}(\Delta_1+\Delta_2+1)\right)\left(\Gamma(\beta)\Gamma\left(-h-\frac{\beta}{2}+1\right)\Gamma\left(-h-\frac{\beta}{2}+\frac{3}{2}\right)\right)}{\Gamma(\Delta_1)\Gamma(-2h-\beta+\Delta_2+2)}}.$$

Finally, putting all back together and choosing $\alpha=\Delta_2$, $\beta=\Delta_1$ for symmetry reasons we get:

$$a_N=\frac{\pi^{d/2}2^{-2\Delta_1-4N-1}(\Delta_2)_{2N}\left(\Delta_1\right)_{2N}\left(-d-\Delta_2+2\right)_{\Delta_1}}{N!\left(\frac{3-d}{2}-\right)_{2N+\Delta_1}},\quad b_N=\frac{\pi^{d/2}2^{-2\Delta_2-4N-1}(\Delta_1)_{2N}\left(\Delta_2\right)_{2N}\left(-d-\Delta_1+2\right)_{\Delta_2}}{N!\left(\frac{3-d}{2}\right)_{2N+\Delta_2}}.\tag{C.3}$$

D Formulas and integrals

$$\frac{1}{A^nB^m}=\frac{\Gamma(n+m)}{\Gamma(n)\Gamma(m)}\int_0^1 dx\frac{x^{n-1}(1-x)^{m-1}}{\left[xA+(1-x)B\right]^{n+m}}\tag{D.1}$$

$$\int\frac{d^d\ell}{(2\pi)^d}\frac{\ell^{2p}}{\left[\ell^2-\Delta\right]^n}=\frac{i(-1)^{n+p}\Gamma\left(\frac{d}{2}+p\right)\Gamma\left(n-p-\frac{d}{2}\right)}{(4\pi)^{\frac{d}{2}}\Gamma\left(\frac{d}{2}\right)\Gamma(n)}\Delta^{\frac{d}{2}+p-n}\tag{D.2}$$

$$\frac{1}{(2(1+2z))^a}{}_2F_1\left(\frac{a}{2},\frac{a+1}{2},a+\frac{3}{2}-b,\frac{1}{(1+2z)^2}\right)=\frac{1}{z^a}{}_2F_1\left(a,1+a-b,2+2a-2b,-\frac{1}{z}\right)\tag{D.3}$$

References

[1] Marco Billò et al. "Defects in conformal field theory". In: *JHEP* 04 (2016), p. 091. DOI: 10.1007/JHEP04(2016)091. arXiv: 1601.02883 [hep-th].

[2] Dalimil Mazáč, Leonardo Rastelli, and Xinan Zhou. "An analytic approach to BCFTd". In: *Journal of High Energy Physics* 2019.12 (Dec. 2019). DOI: 10.1007/jhep12(2019)004. URL: https://doi.org/10.1007%2Fjhep12%282019%29004.

[3] Martin Ammon and Johanna Erdmenger. *Gauge/Gravity Duality: Foundations and Applications*. Cambridge University Press, 2015. DOI: 10.1017/CBO9780511846373.

[4] L. Hoffmann, A. C. Petkou, and W. Ruehl. *Aspects of the conformal operator product expansion in AdS/CFT correspondence*. 2000. arXiv: hep-th/0002154 [hep-th].

[5] Pablo Minces and Victor O. Rivelles. "Scalar field theory in the AdS/CFT correspondence revisited". In: *Nuclear Physics B* 572.3 (Apr. 2000), pp. 651–669. DOI: 10.1016/s0550-3213(99)00833-0. URL: https://doi.org/10.1016%2Fs0550-3213%2899%2900833-0.

[6] Joao Penedones. "Writing CFT correlation functions as AdS scattering amplitudes". In: *Journal of High Energy Physics* 2011.3 (Mar. 2011). DOI: 10.1007/jhep03(2011)025. URL: https://doi.org/10.1007%2Fjhep03%282011%29025.

[7] Edward Witten. *Multi-Trace Operators, Boundary Conditions, And AdS/CFT Correspondence*. 2002. arXiv: hep-th/0112258 [hep-th].

[8] Slava Rychkov. *EPFL Lectures on Conformal Field Theory in $D \geq 3$ Dimensions*. Springer International Publishing, 2017. DOI: 10.1007/978-3-319-43626-5. URL: https://doi.org/10.1007%2F978-3-319-43626-5.

[9] David Simmons-Duffin. *TASI Lectures on the Conformal Bootstrap*. 2016. arXiv: 1602.07982 [hep-th].

[10] D.M. McAvity and H. Osborn. "Energy-momentum tensor in conformal field theories near a boundary". In: *Nuclear Physics B* 406.3 (Oct. 1993), pp. 655–680. DOI: 10.1016/0550-3213(93)90005-a. URL: https://doi.org/10.1016%2F0550-3213%2893%2990005-a.

[11] Pedro Liendo, Leonardo Rastelli, and Balt C. van Rees. "The bootstrap program for boundary CFT d". In: *Journal of High Energy Physics* 2013.7 (July 2013). DOI: 10.1007/jhep07(2013)113. URL: https://doi.org/10.1007%2Fjhep07%282013%29113.

[12] Leonardo Rastelli and Xinan Zhou. "The Mellin Formalism for Boundary CFT$_d$". In: *JHEP* 10 (2017), p. 146. DOI: 10.1007/JHEP10(2017)146. arXiv: 1705.05362 [hep-th].

[13] Agnese Bissi, Tobias Hansen, and Alexander Söderberg. "Analytic Bootstrap for Boundary CFT". In: *JHEP* 01 (2019), p. 010. DOI: 10.1007/JHEP01(2019)010. arXiv: 1808.08155 [hep-th].

[14] Pedro Liendo, Leonardo Rastelli, and Balt C. van Rees. "The Bootstrap Program for Boundary CFT$_d$". In: *JHEP* 07 (2013), p. 113. DOI: 10.1007/JHEP07(2013)113. arXiv: 1210.4258 [hep-th].

[15] Ofer Aharony et al. "Loops in AdS from conformal field theory". In: *Journal of High Energy Physics* 2017.7 (July 2017). DOI: 10.1007/jhep07(2017)036. URL: https://doi.org/10.1007%2Fjhep07%282017%29036.

[16] Sheer El-Showk and Kyriakos Papadodimas. "Emergent spacetime and holographic CFTs". In: *Journal of High Energy Physics* 2012.10 (Oct. 2012). DOI: 10.1007/jhep10(2012)106. URL: https://doi.org/10.1007%2Fjhep10%282012%29106.

[17] Eliot Hijano et al. "Witten diagrams revisited: the AdS geometry of conformal blocks". In: *Journal of High Energy Physics* 2016.1 (Jan. 2016). DOI: 10.1007/jhep01(2016)146. URL: https://doi.org/10.1007%2Fjhep01%282016%29146.

[18] Hong Liu. "Scattering in anti–de Sitter space and operator product expansion". In: *Physical Review D* 60.10 (Oct. 1999). DOI: 10.1103/physrevd.60.106005. URL: https://doi.org/10.1103%2Fphysrevd.60.106005.

[19] Idse Heemskerk et al. "Holography from conformal field theory". In: *Journal of High Energy Physics* 2009.10 (Oct. 2009), pp. 079–079. DOI: 10.1088/1126-6708/2009/10/079. URL: https://doi.org/10.1088%2F1126-6708%2F2009%2F10%2F079.

[20] Luis F. Alday, Johan Henriksson, and Mark van Loon. "An alternative to diagrams for the critical O(N) model: dimensions and structure constants to order 1/N2". In: *Journal of High Energy Physics* 2020.1 (Jan. 2020). DOI: 10.1007/jhep01(2020)063. URL: https://doi.org/10.1007%2Fjhep01%282020%29063.

[21] Charlotte Sleight and Massimo Taronna. "Spinning Mellin Bootstrap: Conformal Partial Waves, Crossing Kernels and Applications". In: *Fortschritte der Physik* 66.8-9 (July 2018), p. 1800038. DOI: 10.1002/prop.201800038. URL: https://doi.org/10.1002%2Fprop.201800038.

[22] Marco Billò et al. "Defects in conformal field theory". In: *Journal of High Energy Physics* 2016.4 (Apr. 2016), pp. 1–56. DOI: 10.1007/jhep04(2016)091. URL: https://doi.org/10.1007%2Fjhep04%282016%29091.

[23] Dalimil Mazac, Leonardo Rastelli, and Xinan Zhou. *A Basis of Analytic Functionals for CFTs in General Dimension*. 2021. arXiv: 1910.12855 [hep-th].

[24] João Penedones. "TASI Lectures on AdS/CFT". In: *New Frontiers in Fields and Strings*. WORLD SCIENTIFIC, Nov. 2016. DOI: 10.1142/9789813149441_0002. URL: https://doi.org/10.1142%2F9789813149441_0002.

[25] D.M. McAvity and H. Osborn. "Conformal field theories near a boundary in general dimensions". In: *Nuclear Physics B* 455.3 (Sept. 1995), pp. 522–576. DOI: 10.1016/0550-3213(95)00476-9. URL: https://doi.org/10.1016%2F0550-3213%2895%2900476-9.

[26] Apratim Kaviraj and Miguel F. Paulos. *The Functional Bootstrap for Boundary CFT*. 2019. arXiv: 1812.04034 [hep-th].

[27] A. Liam Fitzpatrick et al. "Effective conformal theory and the flat-space limit of AdS". In: *Journal of High Energy Physics* 2011.7 (July 2011). DOI: 10.1007/jhep07(2011)023. URL: https://doi.org/10.1007%2Fjhep07%282011%29023.